



SAPIENZA  
Università di Roma  
Facoltà di Scienze Matematiche Fisiche e Naturali

DOTTORATO DI RICERCA  
IN BIOLOGIA CELLULARE E DELLO SVILUPPO

PH. D. IN CELL AND DEVELOPMENTAL BIOLOGY

Cycle: **XXXI**  
(A.Y.: **2017/2018**)

**Analysis of the R451C Neuroligin3 Knock-In mouse, a  
model of a monogenic form of autism**

Ph. D. Student  
**Laura Trobiani**

Supervisor  
Dr. Antonella De Jaco

Coordinator  
**Prof. Giulia De Lorenzo**

## INDEX

<i>Abstract</i>	<b>3</b>
<i>Sommario</i>	<b>5</b>
<i>General Introduction</i>	<b>7</b>
<i>Aims of the work</i>	<b>13</b>
<b>CHAPTER I:</b>	<b>15</b>
<i>UPR activation specifically modulates glutamate neurotransmission in the cerebellum of a mouse model of autism</i>	<b>15</b>
<b>CHAPTER II:</b>	<b>27</b>
<i>Screening of chemical compounds to restore the defective trafficking of R451C Neuroligin3</i>	<b>27</b>
<b>Introduction</b>	<b>27</b>
<b>Results</b>	<b>31</b>
<b>Discussion</b>	<b>47</b>
<b>Methods</b>	<b>53</b>
<b>References</b>	<b>59</b>
<b>Supplementary</b>	<b>69</b>
<i>General conclusions and perspectives</i>	<b>71</b>
<b>LIST OF PUBLICATIONS</b>	<b>77</b>

## Abstract

Autism Spectrum Disorders (ASDs) are neurodevelopmental syndromes, in which several environmental risk factors act on a vulnerable genetic background. Among genes whose mutations have been associated with ASDs, the R451C substitution in the synaptic protein Neuroligin3 (NLGN3) has been highly characterized.

It is known from *in vitro* studies, that the mutation affects folding of the extracellular domain of the protein, causing its retention in the Endoplasmic Reticulum (ER) and the activation of the Unfolded Protein Response (UPR). It has been shown both *in vitro* and *in vivo*, that only ~10% of the mutant protein reach the synapse, causing loss of NLGN3 on the cell surface and leading to alterations in synaptic neurotransmission.

In this work, we have evaluated whether UPR was activated *in vivo*, in the brain of the knock-in mouse model carrying the R451C mutation in the endogenous NLGN3. We showed a selective increase of UPR markers levels in the cerebellum of the R451C mice, along with an increase in the frequency of the miniature excitatory currents in the Purkinje cells, that resulted to be UPR-dependent.

At the same time, in order to find a strategy to rescue NLGN3 folding and expression on the cell surface, we have generated and characterized a new cell-based model system that allowed studying NLGN3 protein trafficking. By using this system, we have screened an FDA-approved library of compounds for improving impaired protein folding. Among the compounds that have been tested, several members of the glucocorticoid

family showed efficacy in increasing mutant protein trafficking and restoring membrane localization.

Collectively, our data indicated that the ER-retention of R451C NLGN3 *in vivo*, caused UPR activation and alterations of synaptic function in the cerebellum of a mouse model of a monogenic form of autism. Furthermore, we identified compounds improving NLGN3 folding and rescuing impaired trafficking.

## Sommario

Negli ultimi anni, un sempre maggior numero di mutazioni associate ai Disturbi dello Spettro Autistico (DSA) è stato rinvenuto in proteine coinvolte nella formazione e nella funzione delle sinapsi, come la famiglia delle proteine post-sinaptiche *Neuroligins* (NLGNs). In particolare, la mutazione R451C in NLGN3 causa un parziale malripiegamento del dominio extracellulare della proteina, portando al suo trattenimento nel Reticolo Endoplasmatico (RE). L'accumulo nel RE della proteina R451C NLGN3, *in vitro*, causa attivazione dell'*Unfolded Protein Response* (UPR) ed è noto che l'espressione di questa proteina mutata porta ad alterazioni delle funzioni sinaptiche in diverse aree cerebrali.

In questo lavoro abbiamo investigato l'attivazione dell'UPR in un modello murino di autismo che esprime in maniera endogena la proteina R451C NLGN3. I nostri dati mostrano attivazione di tale risposta cellulare in maniera specifica nel cervelletto dei topi R451C KI ed un aumento della frequenza della corrente eccitatoria spontanea nelle cellule del Purkinje, che è dipendente dall'attivazione della UPR.

In parallelo, al fine di trovare una strategia per recuperare il corretto ripiegamento della proteina mutata e la sua espressione sulla superficie cellulare, abbiamo generato e caratterizzato un nuovo sistema modello cellulare che ci ha permesso di studiare il *trafficking* di R451C NLGN3 e di effettuare lo *screening* di una libreria di composti approvati dalla *Food and Drug Administration* americana. Tra i composti testati, diversi membri della famiglia dei glucocorticoidi sembravano in grado di aumentare il

*trafficking* e la localizzazione in membrana della proteina R451C NLGN3.

Complessivamente, i nostri dati indicano che la mutazione R451C in NLGN3 porta all'attivazione dell'UPR *in vivo*, nel cervelletto di un topo modello di autismo, dove provoca alterazioni delle funzioni sinaptiche. Inoltre, abbiamo identificato un gruppo di composti in grado di ripristinare il corretto ripiegamento della proteina mutata e il suo traffico sulla superficie cellulare in un sistema modello *in vitro*.

## **General Introduction**

Autism Spectrum Disorders (ASDs) are a group of congenital developmental impairments of the central nervous system (Kawada et al., 2018), which are characterized by abnormal behaviour and communication skills emerging during childhood. Approximately, 1% of children are affected by ASDs, with a male:female ratio of 4:1 (de la torre-Ubieta et al., 2016).

The strong heterogeneity in both genetic and environmental risk factors associated with these syndromes makes difficult to understand their etiology.

In the last years, more than five hundred genetic variants have been correlated with ASDs (Campisi et al., 2018). It is noteworthy that there are several affected cellular pathways among which the synaptic one. In fact, several susceptibility genes codify for synaptic proteins, highlighting that alterations in formation and function of the synapse play a major role in the development of psychiatric and neurological disorders (Taoufik et al., 2018; Ribeiro et al., 2018). Moreover, several environmental factors can act on this genetically vulnerable background to contribute to the ASDs pathogenesis (Li et al., 2012; Campisi et al., 2018).

Among the synaptic genes, a relevant role belongs to the Neuroligins (NLGNs) family of proteins. The post-synaptic NLGNs play a role in the stabilization and function of the synapse through the formation of a trans-synaptic bridge with pre-synaptic partner proteins of the Neurexins (NRXNs) family (Sudhof, 2008; Bang and Owczarek, 2013). NLGNs form a not-covalent homo- or heterodimer, whose interaction with NRXNs is regulated by several factors, such as

alternative splicing, glycosylation state and presence of Ca<sup>2+</sup> ions (Fabrichny et al., 2007).

In humans, the NLGNs family comprises five members, whose genes are located on different chromosomes: *NLGN1* (3q26), *NLGN2* (17p13), *NLGN3* (Xq13), *NLGN4* (Xp22.3) and *NLGN5* (also known as *NLGN4Y*).

The NLGNs show a non-overlapping distribution in the central nervous system, with *NLGN1* at excitatory synapses and *NLGN2* and *NLGN4* at inhibitory synapses. Only *NLGN3* makes an exception, since it is expressed on both types of synapses (Bemben et al., 2015). Little is known about *NLGN5*, which is not expressed in rodents.

Among the NLGNs genes, the highest number of ASDs-associated mutations have been found in *NLGN3* and *NLGN4* (Jamain et al., 2003; Talebizadeh et al., 2006; Yan et al., 2005), though several mutations in ASDs patients have been recently mapped on *NLGN1* gene (Nakanishi et al., 2017).

The most characterized ASDs-associated mutation in the NLGNs family is a point mutation, resulting in a Cys substitution of an Arg residue at position 451 (R451C) in the extracellular protein domain of *NLGN3*. This mutation has been found in two Swedish brothers, one with autism and one with Asperger syndrome (Jamain et al., 2003).

Studies conducted *in vitro* have shown that the R451C mutation affects protein folding and causes partial retention of *NLGN3* in the Endoplasmic Reticulum (ER), leading to its degradation via proteasome (De Jaco et al., 2010). Moreover, it has been shown that the amount of R451C *NLGN3* reaching the cell surface shows reduced binding to its pre-synaptic partner *NRX1β* (Comoletti et al., 2004).

The accumulation of misfolded proteins in the ER can

generate a cellular stress condition, which can trigger a complex signalling, the Unfolded Protein Response (UPR). This response activates transcription of target genes in the nucleus, with the aim to restore ER homeostasis (Chambers and Marciniak, 2014; Almanza et al., 2018).

The UPR comprises three branches: PERK, IRE1 and ATF6. The first line of response is mediated by PERK, which inhibits general protein synthesis by direct phosphorylation of the translation factor eIF2 $\alpha$  (McQuiston and Diehl, 2018). Moreover, IRE1, through its endonuclease activity, mediates the alternative splicing of the transcription factor XBP1, generating its active form (XBP1s) (Ni et al., 2018). Furthermore, in response to ER stress, ATF6 undergoes proteolytic cleavage, generating a transcription factor, ATF6n, which activates transcription of XBP1 and other UPR target genes (Hillary and FitzGerald, 2018).

Besides the role played by UPR in pathological conditions, UPR targets have been recently implicated in the regulation of neuronal physiology (Martinez et al., 2018). For instance, it has been demonstrated that the axis IRE1-XBP1 plays a role in memory formation, through the transcriptional activation of BDNF (Martinez et al., 2016). Moreover, the regulation of protein synthesis mediated by PERK-eIF2 $\alpha$  is implicated in synaptic plasticity (Di Prisco et al., 2014).

Several studies have associated UPR activation with neurodegenerative diseases, such as Alzheimer's, Parkinson's and prion diseases (Mercado et al., 2016; Roussel et al., 2013), but little is known about the correlation between UPR and neurodevelopmental disorders. Only recently, Kawada and Mimori showed an up-regulation of UPR markers in the brain of mice born from VPA-injected mothers (Kawada and

Mimori, 2018). Valproic acid (VPA) administration during pregnancy is a known risk factor of ASDs pathogenesis in the offspring (Christensen et al., 2013). In the same year, Crider and colleagues found increased levels of UPR markers in the middle frontal cortex of ASDs patients (Crider et al., 2017). These data are indicating a possible role of ER stress and UPR activation in the pathogenesis of ASDs. In this context, our group has focused on studying UPR activation triggered by the R451C NLGN3 mutant protein. We have shown activation of all UPR branches in neuronal-like cells stably expressing R451C NLGN3 (Ulbrich et al., 2016). In particular, we have analysed both the activation state of the three UPR effectors and the expression levels of ER chaperones, such as BiP and GRP94, which are commonly up-regulated following UPR activation. Our work has correlated, for the first time, an ASDs-associated mutation to ER stress, putting the basis for further studies on the effects of UPR activation *in vivo*, in the context of the monogenic form of ASDs due to the mutation R451C in NLGN3.

In 2007, the research group headed by prof. Südhof has generated a knock-in (KI) mouse carrying the R451C mutation in the endogenous *NLGN3* gene (Tabuchi et al., 2007). This is considered a model of a monogenic form of ASDs, since it shows ASDs-like behaviours and alterations of synaptic neurotransmission in several brain areas, such as hippocampus, cerebral cortex and dorsal striatum (Tabuchi et al., 2007; Etherton et al., 2011; Martella et al., 2018).

This KI mouse model is a useful tool for studying the effects of the human R451C NLGN3 mutation *in vivo* and to test possible treatment for the monogenic form of ASDs caused by it. Indeed, a crucial issue of ASDs is the lack of appropriate

cures, mostly due to its heterogeneity. Treatments developed so far act only at alleviating symptoms, such as aggressive behaviour and lack of attention. These pharmacological treatments are usually supported by psychological therapy, aiming at improving language and social communication. A better understanding of ASDs etiology would be the first step in developing targeted treatments solving the cause rather than the symptoms.

In the last years, several studies aimed at developing treatments both for protein misfolding and attenuation of UPR activation using both *in vitro* and *in vivo* disease model systems. Some of them reached the stage of clinical trials in some cases of cancer and amyloidogenic diseases (Cortez and Sim, 2014; Valenzuela et al., 2016, 2018; Almanza et al., 2018).

In the context of misfolded proteins, the proteostatic function of chaperones, makes them a tempting therapeutic tool. Whereas molecular and chemical chaperones play a role at helping any other protein to fold, pharmacological chaperones are molecules specifically design to bind a protein of interest and induce its refolding (Cortez and Sim, 2014).

On the other hand, in the last years many pharmacological and gene therapy approaches have been developed to modulate each UPR effector. At the moment, this research field is pointing at better understand the biochemical interaction between UPR factors and drug modulators, with the aim to generate more and more specific treatments (Almanza et al., 2018).

The above-mentioned strategies would represent valid approaches to contrast the effects of the R451C mutation in NLGN3, with the result of both restoring proper protein

localization and favouring protein escape from the ER. Moreover, reducing the ER overload, would alleviate UPR activation and mitigate its downstream effects on neuronal physiology and function.

To conclude, finding molecules specifically helping protein folding would represent an avenue for treating diseases characterized by loss of function due to protein misfolding, or to diseases characterized by gain of function effects due to the retention of the misfolded protein in the ER.

## **Aims of the work**

Among the susceptibility genes whose mutations have been correlated to Autism Spectrum Disorders (ASDs), our interest is focused on the Neuroligins (NLGNs) family. NLGNs are postsynaptic cell-adhesion molecules interacting with a presynaptic partner of the Neurexins (NRXNs) family and supporting synapse formation and function.

The most studied ASDs-associated mutation in NLGNs is the Arg451 to Cys (R451C) substitution in NLGN3. From *in vitro* studies, it is known that the mutation causes a misfolding of the extracellular protein domain, leading to a partial retention of NLGN3 in the Endoplasmic Reticulum (ER), to the activation of the Unfolded Protein Response (UPR) and its degradation through the proteasome.

The generation of the knock-in (KI) mouse carrying the R451C substitution in the endogenous NLGN3 has allowed studying the effects of the mutation *in vivo*. The R451C KI mouse shows autistic-like behaviors and alterations of the synaptic neurotransmission in several brain areas, causing an excitatory/inhibitory imbalance, which is considered a hallmark of autism.

In this thesis, we pursued two principal aims. The first aim was to better characterize the R451C KI mouse model. In particular, we aimed to further analyze both WT and R451C NLGN3 protein expression and degradation *in vivo*. Moreover, we sought to verify whether the mutant protein was retained in the ER and was able to induce UPR activation in a specific brain region of the R451C KI mouse.

And whether UPR was activated, in one or more brain regions that we analyzed, we would evaluate electrophysiological

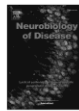
properties of those regions, since it is known from literature data that UPR can modulate synaptic transmission.

The second aim of this thesis was to investigate for a strategy to restore correct protein folding of R451C NLGN3, in order to favor its escape from the ER and to rescue its proper localization on the cell surface and reduce the ER overload. To this purpose, we generated and characterized a new cell-based model system for screening a library of compounds approved by the American Food and Drug Administration (FDA) for improving protein trafficking and restoring proper protein localization and possibly lower UPR activation.



Contents lists available at ScienceDirect

Neurobiology of Disease

journal homepage: [www.elsevier.com/locate/ynbdi](http://www.elsevier.com/locate/ynbdi)

## UPR activation specifically modulates glutamate neurotransmission in the cerebellum of a mouse model of autism

L. Trobiani<sup>a,1</sup>, F.L. Favaloro<sup>b,1</sup>, M.A. Di Castro<sup>b</sup>, M. Di Mattia<sup>b</sup>, M. Cariello<sup>a</sup>, E. Miranda<sup>a,c</sup>, S. Cranerini<sup>d</sup>, M.E. De Stefano<sup>b</sup>, D. Comoletti<sup>d</sup>, C. Limatola<sup>b,e,f</sup>, A. De Jaco<sup>a,g</sup><sup>a</sup> Department Biology and Biotechnologies “Charles Darwin”, Sapienza University of Rome, Center for Research in Neurobiology Daniel Boveri, 00185 Rome, Italy.<sup>b</sup> Department of Physiology and Pharmacology, Sapienza University of Rome, 00185 Rome, Italy.<sup>c</sup> Department of Psychology, Section of Neuroscience, Center for Research in Neurobiology Daniel Boveri, Sapienza University of Rome, 00185 Rome, Italy.<sup>d</sup> Department of Neuroscience and Cell Biology, Department of Pediatrics, Child Health Institute of New Jersey, Rutgers, Robert Wood Johnson Medical School, New Brunswick, NJ, USA<sup>e</sup> Istituto Pasteur Italia Fondazione Cenci Bolognini, Italy.<sup>f</sup> IRCCS Neuromed, Pozzilli (IS), Italy

## ARTICLE INFO

## Keywords:

Neuroigin3

ER stress

Unfolded protein response

Autism spectrum disorders

R451C knock-in mice

Cerebellum

Miniature excitatory post-synaptic currents

BIP

IRE1L

eIF2α

## ABSTRACT

An increasing number of rare mutations linked to autism spectrum disorders have been reported in genes encoding for proteins involved in synapse formation and maintenance, such as the post-synaptic cell adhesion proteins neuroligins. Most of the autism-linked mutations in the neuroligin genes map on the extracellular protein domain. The autism-linked substitution R451C in Neuroligin3 (NLGN3) induces a local misfolding of the extracellular domain, causing defective trafficking and retention of the mutant protein in the endoplasmic reticulum (ER). The activation of the unfolded protein response (UPR), due to misfolded proteins accumulating in the ER, has been implicated in pathological and physiological conditions of the nervous system. It was previously shown that the over-expression of R451C NLGN3 in a cellular system leads to the activation of the UPR. Here, we have investigated whether this protective cellular response is detectable in the knock-in mouse model of autism endogenously expressing R451C NLGN3. Our data showed up-regulation of UPR markers uniquely in the cerebellum of the R451C mice compared to WT littermates, at both embryonic and adult stages, but not in other brain regions. Miniature excitatory currents in the Purkinje cells of the R451C mice showed higher frequency than in the WT, which was rescued inhibiting the PERK branch of UPR.

Taken together, our data indicate that the R451C mutation in neuroligin3 elicits UPR *in vivo*, which appears to trigger alterations of synaptic function in the cerebellum of a mouse model expressing the R451C autism-linked mutation.

## 1. Introduction

Autism spectrum disorders (ASDs) are neurodevelopmental syndromes characterized by a strong heritable component. The genetic underlying ASDs is very heterogeneous, with hundreds of alterations affecting molecular pathways converging on common cellular processes (Abrahams and Geschwind, 2008). However, the generation of numerous mouse models of ASDs has allowed genetic, molecular,

functional and behavioral phenotypes to be investigated as a whole (de la Torre-Ubieta et al., 2016). ASDs high risk penetrance genes comprise those directly involved in brain development (De Ruibus et al., 2014), with genes involved in synaptic function and structure representing the main affected pathways that contribute to ASDs pathogenesis (Bourgeron, 2015; Wang et al., 2017). Among these, the post-synaptic cell-adhesion proteins of the Neuroligin family act as synaptic organizers, involved in the specification of the identity of the synapse and its

**Abbreviations:** NLGN3, neuroligin3; ASDs, autism spectrum disorders; UPR, unfolded protein response; ER, endoplasmic reticulum; WT, wild type; mEPSC, miniature excitatory post-synaptic currents; DMSO, dimethyl sulfoxide; ATF6, activating transcription factor 6; BIP, immunoglobulin heavy-chain-binding protein; eIF2α, eukaryotic initiation factor; PERK, PKR (dsRNA-dependent protein kinase)-like endoplasmic reticulum kinase; IRE1, inositol-requiring enzyme 1; VGLUT, vesicular glutamate transporter; EndoH, endoglycosidase H; HRP, horseradish peroxidase

\* Corresponding author at: Department of Biology and Biotechnologies “Charles Darwin”, Sapienza University of Rome, P.le Aldo Moro 5, Roma 00185, Italy.

E-mail address: [antonella.dejaco@uniroma1.it](mailto:antonella.dejaco@uniroma1.it) (A. De Jaco).

<sup>1</sup> These authors equally contributed to this work.

<https://doi.org/10.1016/j.nbd.2018.08.026>

Received 27 February 2018; Received in revised form 1 August 2018; Accepted 30 August 2018

Available online 07 September 2018

0969-9961/ © 2018 Elsevier Inc. All rights reserved.

functional maturation (Baig et al., 2017). The Neuroligin (NLGN) family of proteins consists of different members specifically localized to particular synapses. NLGN1 is expressed exclusively at excitatory terminals (Song et al., 1999); NLGN2 and 4 localize at inhibitory synapses (Hoon et al., 2011; Varsquez et al., 2004, 2006), whereas NLGN3 is present in both synapses (Budreck and Scheiffele, 2007). ASDs rare mutations in NLGNs, with NLGN3 and NLGN4 being the most prevalent, have been characterized for their effect as loss or gain of function mutations *in vitro* (Talebizadeh et al., 2006; Zhang et al., 2009) and *in vivo* (Ehretson et al., 2011a, 2011b; Jamain et al., 2008; Radyushkin et al., 2009).

Recently new NLGN1 variants have been reported and characterized, strengthening the involvement of NLGN with ASDs (Nakanishi et al., 2017). However, the *de novo* missense substitution of the arginine 451 to cysteine (R451C) in NLGN3 represents the prototypic mutation, being the first identified in a Swedish family in 2003 (Jamain et al., 2003). Our work and others show that this mutation alters proper folding of the extracellular domain of NLGN3, partially blocking the trafficking of the mutant protein to the cell surface through its retention in the endoplasmic reticulum (ER) (Chih et al., 2004; Comolletti et al., 2004). Several ER chaperones, such as BiP, have been found to participate in the retention of the mutant protein in the ER and in its degradation by the proteasome (De Jaco et al., 2008, 2010a, 2010b). This leads to reduced amount of NLGN3 exported to the dendrites, where it normally interacts with the pre-synaptic partner neuexin, favouring the interaction between pre- and post-synaptic terminals (Südhof, 2008). The knock-in (KI) mouse model with the R451C substitution in the endogenous gene, presents reduced NLGN3 levels in the whole brain, suggesting that the mutation causes protein instability *in vivo*, similarly to what observed *in vitro* (Tabuchi et al., 2007). In addition, the R451C mice manifested autistic-like behaviors and a gain of function in the neuronal circuitry, characterized by a region-specific imbalance in the excitatory/inhibitory neurotransmission, with enhanced glutamatergic currents in the hippocampus and increased GABAergic transmission in the somatosensory cortex. Interestingly, none of these features were observed in the WT or in the Knock Out (KO) strains (Cellot and Cherubini, 2014; Ehretson et al., 2011a; Földy et al., 2013) (Tabuchi et al., 2007). These findings favor the hypothesis that ASDs phenotypes may result from dysfunctional synaptic networks, with alterations in the balance between excitatory and inhibitory synaptic transmission in brain regions involved in the regulation of behavior (Bourgeron, 2009), as found in other ASDs animal models (Lee et al., 2016).

The perturbation of ER homeostasis due to the retention of misfolded proteins appears linked to the etiology of several pathologies of the nervous system (Hetz et al., 2013; Roussel et al., 2013). Stress conditions in the ER induce activation of the unfolded protein response (UPR), a signaling cascade enhancing both protein folding capacity and proteasome-mediated degradation, while attenuating protein synthesis, aiming at reducing the stress in the organelle. The UPR is mediated by three ER-membrane proteins: ATF6 and IRE1 are functioning in the transcriptional activation of UPR-targets such as molecular chaperones; the kinase PERK is directly involved in the phosphorylation of the eukaryotic translation initiation factor eIF2 $\alpha$ , that in turn leads to the attenuation of global protein synthesis (Chambers and Martiniak, 2014). Our group has recently shown that the partial retention of the R451C mutant protein in the ER leads to the activation of all three branches of UPR in the PC12 Tet-on cell lines with inducible expression of NLGN3. The activation was time-dependent from the induction of the synthesis of the mutant protein and resulted in the up-regulation of BiP and in the phosphorylation of eIF2 $\alpha$  (Ulbrich et al., 2016).

In this work, we explored the cellular responses elicited *in vivo* by the ER retention of the R451C mutant protein and the downstream effects on neurotransmission. We show that, *in vivo*, the R451C substitution causes partial retention of the mutant protein in the ER, affecting its post-translation glycosylation processing and favouring its

degradation by the proteasome. More importantly, we report *in vivo* UPR activation in the total brain of the R451C mouse, both at embryonic and adult stages, and we identify the cerebellum as the region where the UPR markers are uniquely up-regulated. Interestingly, inhibition of the PERK signaling branch of the UPR restores altered neurotransmission in cerebellar slices from the R451C mouse, providing a link between modulation of UPR and pre-synaptic neurotransmitter release. These findings indicate, for the first time, an involvement of the UPR in the alteration of neurotransmission in an animal model of a monogenic form of ASDs.

## 2. Methods

### 2.1. Animals and treatments

B6;129-Nlgn3tm1Sud/J knock-in mice (R451C) and parental strain (WT) were a kind gift from Dr. Andrea Barberis (Italian Institute of Technology, Genoa). All experimental procedures were done on littermate mice, obtained from mating either WT or R451C male mice with heterozygous females. Mice were provided with *ad lib* food and water and were kept on a 12h light/12h dark cycle at the temperature of  $20 \pm 1$  °C. Mouse sacrifice was done by cervical dislocation, in accordance to the animal protocol stipulated and to the current Italian law (D.lgs. 26/2014). All experimental procedures and protocols were approved by the Ethical Committee for Animal Research of the Italian Ministry of Public Health (Sapienza University protocol number 0061/2013 and 541/2016-PR).

Mouse genotype was ascertained on the genomic DNA using PCR conditions and primers previously described by (Tabuchi et al., 2007). Unless otherwise specified, most of the experiments were done on adult mice at age P60.

Mice from WT strain injected intraperitoneally with 500  $\mu$ g/kg tunicamycin (#T7765 Sigma-Aldrich, Milan, Italy) 48 h before dissection (Iwawaki et al., 2004; Maheshwari et al., 1983), represented the experimental positive control for inducing ER stress *in vivo*, while DMSO (#D2438 Sigma-Aldrich, Milan, Italy) injection (in 1.5% in PBS) was used as vehicle-control condition.

Proteasome-inhibitor treatments *in vivo* were performed by subcutaneous injections of 5 mg/kg/day of MG132 (Z-Leu-Leu-Leu-al.#C2211 Sigma-Aldrich, Milan, Italy) or with the same volume of PBS (vehicle-control condition) as previously described by (Yan et al., 2014). Injections started from P4 and continued daily up to P20, and the total brain from each mouse was collected 1 h after the last injection at P20.

### 2.2. Protein extraction from mouse tissues

Whole brain and sub-regions (hippocampus, cerebral cortex, cerebellum) were dissected from adult mice and rapidly frozen in dry ice. For every 100 mg of tissue, we used 1.5 ml of lysis buffer: 0.5  $\times$  TBS (10 mM TRIS-HCl pH 7.6, 68.4 mM NaCl), 7.5 mM EDTA, 10 mM EGTA, 1% Triton X-100, added with phosphatase inhibitors (50  $\mu$ M NaF, 1  $\mu$ M Na<sub>3</sub>VO<sub>4</sub>, 1  $\mu$ M PMSF) and protease inhibitor cocktail (Sigma-Aldrich, Milan, Italy). Tissues were sonicated at max 100% amplitude with the Ultrasonic Processor UPI00H (Hielscher, Germany) until the lysate appeared clear and then incubated for 30 min on ice. The soluble fraction was collected after centrifugation at 17,000  $\times$ g for 30 min at 4 °C and diluted four-fold in the lysis buffer for the determination of total proteins concentration by Bradford assay.

### 2.3. SDS-PAGE and western blot analysis

For whole brain and single brain sub-regions, 50  $\mu$ g of total proteins were loaded for detecting NLGN3 and BiP, 25  $\mu$ g for VGLUT1 and 75  $\mu$ g for detecting P-eIF2 $\alpha$ . Approximately 130  $\mu$ g of total proteins from the whole brain lysate, were used to detect NLGN3 levels after MG132

treatments *in vivo*. Loading buffer containing  $\beta$ -mercaptoethanol and sodium dodecyl sulphate (SDS) was added to the lysates before heating at 100 °C for 5 min. Samples were separated on a 10% w/v acrylamide SDS-PAGE in running buffer (25 mM Tris, 20 mM glycine, 3.5 mM SDS) and proteins blotted on Immobilon PVDF membranes (Millipore, through SIAL S.r.l., Italy) in transfer buffer (25 mM Tris, 20 mM glycine, 10% v/v Methanol) as previously described (Canterini et al., 2012; De Jaco et al., 2010b). Membranes were blocked with 5% (w/v) non-fat dried milk powder in TBS added with 0.2% Tween (T-TBS) or with 3% (w/v) bovine serum albumin (BSA, AppliChem Panrec) in PBS (2.68 mM KCl, 1.47 mM  $\text{KH}_2\text{PO}_4$ , 0.137 M NaCl, 10.16 mM  $\text{Na}_2\text{HPO}_4$ ) for the detection of eIF2 $\alpha$  phosphorylation. Primary antibodies were diluted in PBS with 3% BSA and 0.1% NaAz (Sigma-Aldrich, Milan, Italy) at the following dilutions: NLGN1 (1:1000, mouse, #129–111 Synaptic Systems, Goettingen, Germany), NLGN2 (1:1000, rabbit, #129–203, Synaptic Systems, Goettingen, Germany), NLGN3 (1:1000, rabbit, #129–113 Synaptic Systems, Goettingen, Germany), P-eIF2 $\alpha$  (Ser51) (1:1000, rabbit, #119A11 Cell Signaling), total eIF2 $\alpha$  (1:1000, mouse, #L57A5 Cell Signaling, Danvers, Massachusetts, United States), BIP (1:1000, rabbit, #ab53068 Abcam, Cambridge, UK), VGLUT1 (1:1000, #135–303 Synaptic Systems, Goettingen, Germany),  $\beta$ -Actin (1:1000, mouse, #MAB1501 Millipore, through SIAL S.r.l., Italy), PSD95 (1:1000, mouse, #666-1C9 Enzo Life Sciences through 3VChimica S.r.l., Italy) and gephyrin (1:1000, mouse, #147–111 Synaptic Systems, Goettingen, Germany). The HRP (horseradish peroxidase)-conjugated secondary antibodies, goat-anti-mouse-HRP and goat-anti-rabbit-HRP (Sigma-Aldrich, Milan, Italy) were used 1:10000 dilution in 5% (w/v) non-fat dried milk powder in T-TBS and incubated for 1 h. The HRP signal was developed using the LiteAbot PLUS or TURBO extra sensitive chemiluminescent substrates (Euroclone, Milan, Italy) and visualized by a ChemiDoc system (BioRad, Italy). Densitometry was performed on at least three independent experiments using ImageJ software (NIH).

#### 2.4. Digestion with endoglycosidase H

About 20  $\mu\text{g}$  of total proteins extracts from E18 total brains were incubated in denaturing buffer for 10 min at 100 °C. Endoglycosidase H enzyme (1500 enzymatic units, Endo H, New England Biolabs) was added to the reaction buffer at 37 °C for 3 h (De Jaco et al., 2006). Treated and untreated samples were subjected to SDS-PAGE and immunoblotting using the anti-NLGN3 antibody as described above.

#### 2.5. Histology and immunofluorescence

Mice were deeply anesthetized with a mixture of Zoletil-100 (20 mg/Kg b.w.; Virbac, France) and Rompun® (8 mg/Kg b.w.; Bayer, Canada), diluted in saline, and perfused via the ascending aorta with a Ringer solution (145.5 mM NaCl, 16.77 mM KCl, 11.9 mM  $\text{NaHCO}_3$ ), followed by 100 ml of fixative composed of freshly depolymerized 4% paraformaldehyde (PFA, Sigma-Aldrich, Milan, Italy) in 0.1 M phosphate buffer (PB), pH 7.4. Brains were rapidly removed, cryoprotected in a 30% sucrose/saline solution for 2–3 days at 4 °C, frozen on dry ice and stored at –80 °C until use. Cerebellar sagittal serial sections (25  $\mu\text{m}$ ) were cut at a freezing microtome (Leica), collected free floating in 0.1 M PB and processed for immunofluorescence (Amesè et al., 2015; Palladino et al., 2015). After a block in 10% bovine serum albumin (BSA), 10% normal goat serum (NGS) and 0.5% Triton X-100 in 0.1 M PBS (for 1 h at RT), the sections were incubated for 2 overnight at 4 °C in a mixture of the primary antibodies: anti-MAP2 (Rabbit, dilution 1:600, #DSG1, Cell Signaling) and anti-KDEL (Mouse, dilution 1:500, #ADI-SPA-827 Enzo Life Sciences, through 3VChimica S.r.l., Italy) diluted in 1% BSA, 1% NGS and 0.2% Triton X-100 in 0.1 M PBS. After a rinse in 0.1 M PBS (3  $\times$  10 min), sections were incubated with a mixture of the respective secondary antibodies: anti-mouse IgG (Alexa 594, 1:2000 Goat, Sigma-Aldrich, Milan, Italy); anti-rabbit IgG (Alexa 488,

1:2000 Goat, Sigma-Aldrich, Milan, Italy), diluted in the same diluent of the primaries. The nuclei were stained for 10 min with Draq5 (Far-Red Fluorescent Live-Cell Permeant DNA Dye, Abcam, Cambridge, UK) diluted 1:1000 in PBS. After a final rinse in 0.1 M PBS (3  $\times$  10 min), sections were collected on glass slides and mounted with Prolong® Gold antifade reagent with DAPI (Life Technologies, Milan, Italy). Images were acquired at Zeiss 780 confocal microscope using a 40  $\times$  objective with 1.9  $\times$  zoom.

At least 4 Z-stack images (interval 3.5  $\mu\text{m}$  for 0.5  $\mu\text{m}$ ) were acquired for each experiment in order to measure KDEL staining intensity. We have analysed the fluorescence intensity for each Purkinje cell using ImageJ software (NIH) and then measured the corrected total cell fluorescence (CTCF) by applying this formula:  $\text{CTCF} = \text{integrated density} - (\text{Area of selected cell} \times \text{Mean fluorescence of background readings})$  as previously described (Sun et al., 2016).

#### 2.6. Real time RT-PCR

Total RNA was extracted from whole brain tissue and sub-regions using Trizol reagent (100 mg tissue/ml of Trizol) and following manufacturer's protocol (Life Technologies, Milan, Italy). Because of the low amount of the starting material (< 30 mg animal tissue) Nucleo-Spin RNAiI kit (Machery-Nagel, through Carlo Erba reagents, Milan, Italy) was used for extracting RNA from the hippocampal samples. RNA was quantified with NanoDrop 2000 spectrophotometer (Thermo Scientific, Milan, Italy) and DNase I turbo treatment (Ambion, Thermo Fisher Scientific, Milan, Italy) was used to avoid genomic DNA contamination. RNA was reverse transcribed into single-stranded cDNA using Superscript II (Life Technologies, Milan, Italy), starting from total RNA concentrations of around 2  $\mu\text{g}$  (or less), according to the amount of RNA extracted. The resulting cDNA was subjected to real-time reverse transcription (RT)-PCR using SYBR Green (Life Technologies, Milan, Italy) and amplified for 40 cycles with 15 s at 95 °C followed by 60 s at 60 °C, as previously described (Camp et al., 2010) in the thermocycler iCycler PCR Detection System (Bio-Rad, Italy). Melting curves were obtained at the end of each amplification run to assess the specificity of each primer set. All assays were run in triplicate and relative gene expression levels were calculated using the comparative Ct method (Livak and Schmittgen, 2001). Primer sequences (Sigma-Aldrich, Milan, Italy): BIP Forward (5'-3')-TATTGGAGGTGGCAACCAAG and Reverse (5'-3')-CGCTGGGCATTTGAAGTAAAG and for  $\beta$ -Actin Forward (5'-3')-TGACAGGATGCAGAGGAGA and Reverse (5'-3')-GTACTTCCCTCA GGAGGAC.

#### 2.7. Electrophysiological recordings

Adult mice were anesthetized with halothane and sacrificed by decapitation. Cerebellum was rapidly removed and placed in an oxygenated ice-cold saline buffer (87 mM NaCl, 75 mM Sucrose, 2 mM KCl, 7 mM  $\text{MgCl}_2$ , 0.5 mM  $\text{CaCl}_2$ , 25 mM  $\text{NaHCO}_3$ , 1.2 mM  $\text{NaH}_2\text{PO}_4$ , 10 mM glucose, pH 7.4, 300–305 mOsm) then cut in transversal slices (350  $\mu\text{m}$ ) by a Thermo Scientific HM 650 V vibrating Microslicer. Slices were incubated in oxygenated artificial cerebrospinal fluid containing 125 mM NaCl, 2 mM KCl, 7 mM  $\text{MgCl}_2$ , 0.5 mM  $\text{CaCl}_2$ , 25 mM  $\text{NaHCO}_3$ , 1.2 mM  $\text{NaH}_2\text{PO}_4$  and 10 mM glucose (pH 7.4, 300–305 mOsm) at room temperature for 1 h, then maintained in this condition or incubated in 400 nM GSK2606414 (Selleck Chemicals, through Aurogene, Rome, Italy) for 2 h (Zimmermann et al., 2018). After incubation, slices were transferred to a recording chamber within 1–6 h after slice preparation or processed for protein extraction.

During electrophysiological recordings, slices were constantly maintained in oxygenated saline or in 400 nM GSK2606414 solution (2–2.5 ml/min perfusion rate). Purkinje neurons were visualized through a 40  $\times$  water-immersion objective. Whole-cell membrane currents were recorded with patch-pipettes having a tip resistance of 2–4 M $\Omega$  and acquired (sampling 10 kHz, low-pass filtered 2 kHz) with

DiGData-1440A using pCLAMP-v10 software (Axon Instruments). Spontaneous miniature excitatory postsynaptic currents (mEPSCs) were recorded after application of TTX 0.5 mM (Tocris Bioscience, Bristol, UK) to block action potentials-dependent neurotransmitter release and Picrotoxin 100  $\mu$ M (Tocris Bioscience, Bristol, UK) to block GABA-mediated currents. mEPSC frequency, amplitude and other parameters were analysed off-line using MiniAnalysis software (Synaptosoft, Decatur) with a mEPSC threshold set at 4.5 pA (2.5 times root mean-square noise).

### 2.8. Statistical analysis

All the experiments were performed at least three times on independent biological samples. The exact number of the replicates is indicated in the text and in the figure legends where *n* refers to the number of mice analysed. The only exception is represented by the electrophysiological experiments (Fig. 5) where *n* refers to the number of patched cells.

In Figs. 2, 3, 4 and 6C, data have been normalized to the mean value of the respective control that, according to each specific experimental plan, could be either WT littermates or vehicle-injected mice of the same genotype.

Either unpaired T-student or one-way ANOVA, as specified in the figure legends, were used for statistical analysis by using Prism5 (Graph-Pad 5 Software Inc.): \**p* < .05, \*\**p* < .01, \*\*\**p* < .001.

## 3. Results

### 3.1. *Neuroigin3* expression in WT and R451C mice

A full characterization of the R451C NLGN3 KI mouse, including synaptic transmission, social behaviors, and protein expression of NLGN3 in the brain of the adult R451C NLGN3 mouse was conducted (Tabuchi et al., 2007), and a key finding was that the amino acid substitution decreases NLGN3 levels by ~90% as measured by quantitative immunoblotting. In agreement with these data, our animals show comparable mRNA levels but a drastic decrease in mutant NLGN3 protein in total brain extracts from adult R451C compared to WT mice (data not shown), confirming that the impact of the mutation on the stability of the protein *in vivo* is similar to what we have shown previously *in vitro* (De Jaco et al., 2010b). Endogenous NLGN3 levels are detectable starting from embryonic stages as early as E12 and increase throughout development to adulthood (Budreck and Scheiffele, 2007). We compared the expression profile of NLGN3 in WT and R451C mice at different embryonic stages, starting from E12. NLGN3 levels increased from E12 to E18 in WT embryos, while in R451C mice a significant reduction occurred from E14 to E18 compared to WT. However, an increasing trend was observed for R451C NLGN3 levels, although it wasn't statistically significant (Fig. 1A). Interestingly, immunoblot of R451C NLGN3 protein extracted from brain before birth (E18) showed two distinct bands of slightly different molecular weights (Fig. 1A, E18 lane), suggesting that N-linked glycosylation is incomplete. The incomplete, or immature, glycosylation was previously resolved in pulse-chase experiments in over-expression studies, in which we showed that the mutation dramatically slowed protein processing through ER and Golgi, where N-linked glycosylation is modified (De Jaco et al., 2010b). We also analysed NLGN3 levels at different post-natal stages (Fig. 1B) and noticed that mutant NLGN3 levels were stable from post-natal day 5 (P5) to P60, being lower than the WT, which increased from P5 to P20 and remained constant up to P60.

To investigate whether the reduced expression of the mutant protein in the total brain of adult mice was region-dependent, we evaluated NLGN3 expression in three brain areas, choosing those areas that have been linked to ASDs in humans: cerebral cortex, hippocampus and cerebellum, and showed that there is no region-dependent reduction in the R451C NLGN3 compared to the WT protein (Fig. 1C).

### 3.2. Endoplasmic reticulum retention and degradation of R451C *Neuroigin3* *in vivo*

By using different cellular model systems, we have previously shown that R451C NLGN3 is partially retained in the ER and the protein is sensitive to endoglycosidase H (endoH) digestion, an enzyme that specifically cleaves high mannose glycans, typically found on proteins transiting in the ER (De Jaco et al., 2010b; Ulbrich et al., 2016). To assess whether the residual amount of R451C mutant protein *in vivo* is retained in the ER, we treated WT and R451C KI total brain extracts from E18 embryos with endoH. At this developmental stage the mutant protein can be detected, in contrast to adult brain stages where the protein is barely visible.

Whereas NLGN3 from WT embryos was, as expected, insensitive to the treatment, R451C NLGN3 showed partial sensitivity to the enzyme, as indicated by the band-shift to a lower migrating band after separation on an SDS gel and analysis by western blot (Fig. 2A). This result confirmed that endogenous R451C NLGN3 is at least partially retained in the ER and contains immature N-linked glycosylation.

The severely reduced levels of R451C NLGN3 protein suggest that the protein may be preferentially degraded through the proteasome, as previously demonstrated *in vitro* (De Jaco et al., 2010b). To test this hypothesis *in vivo*, we injected mice from P4 to P20 with the proteasome inhibitor MG132 (or vehicle) and compared the NLGN3 protein levels in the total brain at the end of the treatment at P20. After MG132 treatment, significant increased levels of NLGN3 were observed only in the brain of R451C mice (Fig. 2B), indicating the preferential degradation of the mutant protein by the proteasome.

### 3.3. Mutant R451C *Neuroigin3* leads to the activation of UPR *in vivo*

Since R451C NLGN3 activated the UPR *in vitro* (Ulbrich et al., 2016), we have studied whether expression of UPR targets is also increased in the brain of the R451C mice. UPR activation was investigated in the total brain from E18 embryos, developmental stage at which R451C NLGN3 is detectable. Using real-time RT-PCR we quantified the expression of the master chaperone BiP, one of the main UPR-induced target genes (Takayanagi et al., 2013), which we have previously reported to be up-regulated *in vitro* (Ulbrich et al., 2016). We found significantly higher BiP messenger levels in the cerebellum of R451C embryos compared to WT (Fig. 3A), but not in the encephalon (Fig. 3A), indicating a region-specific activation of the UPR in R451C mouse.

BiP expression was then investigated in adult mice (P60) in hippocampus, cerebral cortex and cerebellum to assess whether the UPR was maintained in the adulthood. Our data showed that BiP messenger was increased in the cerebellum from R451C mice in comparison to the WT strain, while it was unchanged in the other brain regions (Fig. 3B). Literature data report that primary cultures of cerebellar granule cells (CGCs) are more sensitive to the ER stress inducer tunicamycin in comparison to hippocampal (Kosuge et al., 2006) and cortical neurons (Sun et al., 2013). Based on these observations, we have induced UPR in the brain of WT mice (P60) by tunicamycin injections and analysed BiP messenger levels in the cerebellum and hippocampus. Tunicamycin-treated mice, compared to vehicle-treated controls (1.5% DMSO in PBS), showed higher BiP messenger levels in the cerebellum but not in the hippocampus (Fig. 3C), confirming that the cerebellum is more sensitive to ER stress conditions compared to other brain areas and, as expected, it engages the UPR signaling.

In line with the above results, in the R451C mice BiP protein levels closely matched the mRNA expression profile, with a significant increase in the cerebellum but not in the other brain regions, in comparison to the same brain areas in WT mice (Fig. 4A). We next evaluated the activation of UPR mediators, focusing on the PERK branch, which is implicated in the regulation of learning and memory through the phosphorylation of the eukaryotic translation initiation factor 2 $\alpha$  (eIF2 $\alpha$ ) and the translation of activating transcription factor 4 (ATF4)

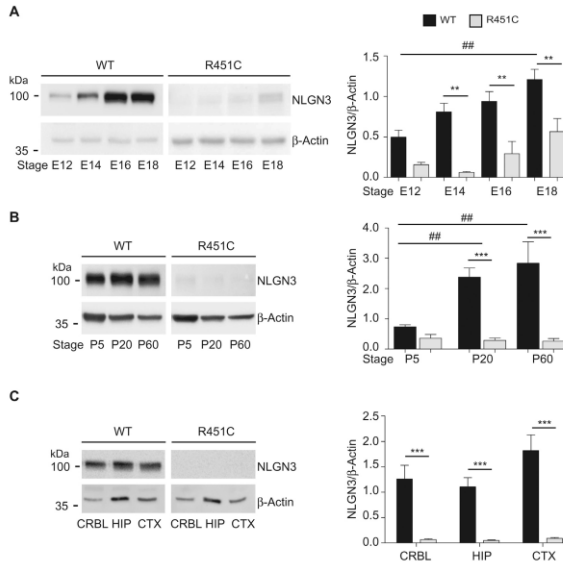


**Fig. 1.** Neuroligin3 protein levels during development in WT and R451C mice. **A.** Representative western blots of WT and R451C brain extracts from E12 to E18 for NLGN3 with relative densitometric analysis comparing R451C versus WT (mean  $\pm$  SEM; E12 WT  $n = 5$ ; E12 R451C  $n = 5$ ; E14 WT  $n = 5$ ; E14 R451C  $n = 6$ ; E16 WT  $n = 6$ ; E16 R451C  $n = 5$ ; E18 WT  $n = 5$ ; E18 R451C  $n = 6$ ;  $^{**}p < .01$ , one-way ANOVA) and E12 versus E18 within the WT condition ( $^{##}p < .01$ ). **B.** NLGN3 brain levels from P5 to P60. Densitometric analysis between WT and R451C at P20 and P60 (mean  $\pm$  SEM; P5 WT  $n = 4$ ; P5 R451C  $n = 5$ ; P20 WT  $n = 9$ ; P20 R451C  $n = 8$ ; P60 WT  $n = 4$ ; P60 R451C  $n = 5$ ;  $^{***}p < .001$  one-way ANOVA) and comparing P5 versus P20, and P5 versus P60 within the WT condition ( $^{##}p < .01$ ). **C.** Representative western blot and densitometric analysis of NLGN3 protein levels in WT and R451C mice in three brain areas involved in autism: cerebellum (CRBL), hippocampus (HIP) and cerebral cortex (CTX). The histogram shows mean  $\pm$  SEM of 8 independent experiments (one-way ANOVA  $^{***}p < .001$ ).

(Hetz and Mollereau, 2014). As shown by our previous work, R451C NLGN3 activates the PERK branch of UPR *in vitro* by increasing the phosphorylation levels of eIF2 $\alpha$  (Ullrich et al., 2016). Consistent with our previous results, mutant R451C NLGN3 mice showed higher levels of phosphorylated eIF2 $\alpha$  (P-eIF2 $\alpha$ ) uniquely in the cerebellum in comparison to WT mice. This increase was not observed for the other brain regions analysed (Fig. 4B).

#### 3.4. Altered excitatory neurotransmission in the cerebellum of R451C Neuroligin3 mice

Induction of ER stress conditions in primary neuronal cultures by tunicamycin was reported to affect spontaneous neurotransmission, specifically by increasing the frequency of the miniature spontaneous excitatory postsynaptic currents (mEPSC) (Nosyreva and Kavalali, 2010). Based on these observations, we have investigated excitatory neurotransmission in the cerebellum of KI adult mice (P60) by recording the mEPSC from cerebellar Purkinje cells (PCs). Our results show that mEPSC amplitude values are similar in R451C and WT slices

(Fig. 5B), whereas mEPSC frequency significantly increased in the R451C slices (Fig. 5C). To test whether the increase of mEPSC frequency was due to increased number of presynaptic terminals in R451C mice, we used VGLUT1 as a marker of the parallel-fiber synapses, indicative of presynaptic terminal density. Our results showed no significant differences in the levels of VGLUT1 between R451C and WT cerebellar tissues (Fig. 5D), suggesting that the increase in mEPSC frequency might be due to an enhanced release probability caused by the activation of the UPR intracellular pathway, as previously shown *in vitro*, rather than a higher number of presynaptic innervations.

In previous work, NLGN1 levels were shown to be modulated in the total brain of the R451C NLGN3 mouse (Tabuchi et al., 2007), therefore we have investigated NLGN1 and NLGN2 protein expression in the cerebellum of KI and WT mice (P60). Interestingly, the R451C mouse presents higher levels of NLGN1 (Fig. 5E) that is normally localized at the excitatory synapses (Song et al., 1999), and unchanged levels of NLGN2 (Fig. 5F) that is found in the inhibitory synapses (Varoqueaux et al., 2004). Additional synaptic markers were also evaluated; in particular PSD95 and gephyrin, post-synaptic density proteins of excitatory

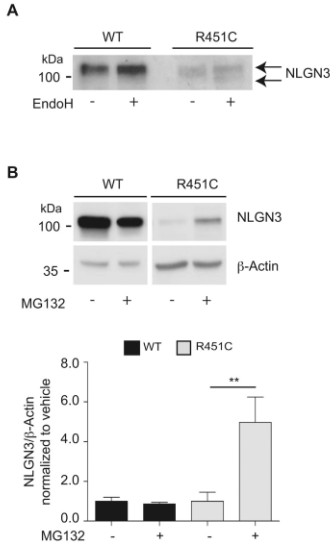


**Fig. 2.** Neuroligin3 glycosylation and degradation. **A.** Western blot of E18 total brain lysates from WT and R451C mice showing differential sensitivity of R451C to WT NLGN3 to endoglycosidase H treatment. **B.** Densitometric analysis of NLGN3 protein levels in total brain extracts from WT and R451C mice treated with the proteasome inhibitor MG132, compared to vehicle-treated control, for each genotype (mean  $\pm$  SEM; WT vehicle  $n = 5$ ; WT MG132  $n = 8$ ; R451C vehicle  $n = 5$ ; R451C MG132  $n = 7$ ; one-way ANOVA  $^{*}P < .01$ ).

and inhibitory synapses respectively. The analysis by western blot showed higher expression of PSD95 in the cerebellum of R451C mice (Supplementary Fig.1A), while gephyrin resulted unchanged (Supplementary Fig.1B). These results confirm the potentiation of the excitatory circuit in the cerebellum of R451C KI mice.

To test whether there is a causal link between activation of UPR and augmentation of excitatory spontaneous neurotransmission, we hypothesized PERK branch activation and phosphorylation of eIF2 $\alpha$  to be involved in the regulation of the synaptic function in response to ER stress. We measured the mEPSC properties after treatment with GSK2606414, a specific inhibitor of PERK, and found that the pharmacological treatment applied to R451C cerebellar slices decreased mEPSC frequency to WT levels (Fig. 6A). Moreover, the frequency of mEPSC was nearly rescued to the values of the untreated condition, by a 30 min-wash of the R451C KI slices previously incubated with GSK2606414. (data not shown). At the same time, significant decrease of mEPSC amplitude was detected in R451C slices after GSK2606414 treatment (Fig. 6B). To confirm that GSK2606414 treatment was inhibiting eIF2 $\alpha$  phosphorylation, cerebellar slices subjected to the same experimental conditions as those used for the electrophysiological recordings were collected for western blot analysis. As shown in Fig. 6C,

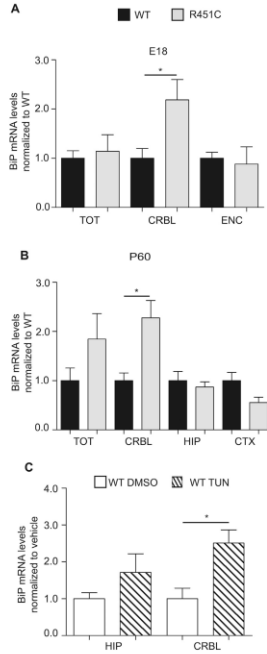


**Fig. 3.** BIP messenger levels in WT and R451C mice at E18 and P60. **A.** Analysis of BIP mRNA levels in embryonic total brain (TOT), cerebellum (CRBL) and encephalon (ENC) from WT and R451C mice at E18 (mean  $\pm$  SEM; TOT WT  $n = 8$ ; TOT R451C  $n = 8$ ; CRBL WT  $n = 14$ ; CRBL R451C  $n = 9$ ; ENC WT  $n = 3$ ; ENC R451C  $n = 3$ ; one-way ANOVA  $^{*}P < .05$ ). **B.** Levels of BIP mRNA in adult brain regions from WT and R451C mice at P60 (TOT: Total brain; CRBL: cerebellum; HIP: hippocampus; CTX: cerebral cortex). Mean  $\pm$  SEM; TOT WT  $n = 10$ ; TOT R451C  $n = 7$ ; CRBL WT  $n = 9$ ; CRBL R451C  $n = 13$ ; HIP WT  $n = 6$ ; HIP R451C  $n = 7$ ; CTX WT  $n = 6$ ; CTX R451C  $n = 6$ ; one-way ANOVA  $^{*}P < .05$ . **C.** BIP mRNA levels in the hippocampus (HIP) and cerebellum (CRBL) of WT adult mice after injection with tunicamycin. Bar-graph shows mean  $\pm$  SEM; HIP WT DMSO  $n = 7$ ; HIP WT TUN  $n = 4$ ; CRBL WT DMSO  $n = 4$ ; CRBL WT TUN  $n = 5$ ; one-way ANOVA  $^{*}P < .05$ .

GSK2606414 significantly reduced P-eIF2 $\alpha$  levels only in cerebellar slices from R451C mice.

These results strongly indicate that the probability of glutamate release in the R451C mice is increased in the excitatory connections to PCs and that these alterations may be linked to the activation of UPR.

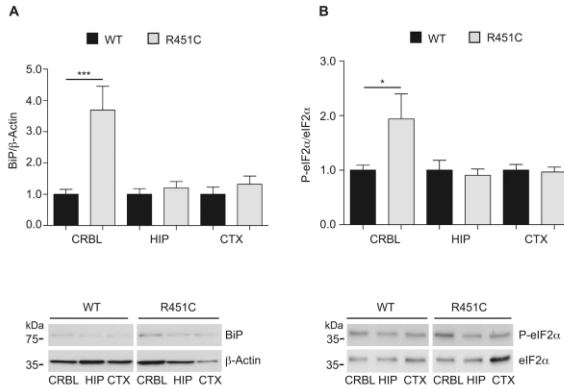


**Fig. 4.** UPR activation in the brain of adult R451C mice. **A.** BiP protein levels in total brain (TOT), cerebellum (CRBL), hippocampus (HIP) and cerebral cortex (CTX) of WT and R451C adult mice normalized to  $\beta$ -actin, mean  $\pm$  SEM; CRBL WT n = 5; CRBL R451C n = 6; HIP WT n = 6; HIP R451C n = 6; CTX WT n = 6; CTX R451C n = 6; one-way ANOVA  $^{***}P < .001$ . **B.** Densitometric analysis and representative western blot for P-eIF2 $\alpha$  normalized to total eIF2 $\alpha$  in brain regions from WT and R451C adult mice, mean  $\pm$  SEM; CRBL WT n = 7; CRBL R451C n = 5; HIP WT n = 7; HIP R451C n = 7; CTX WT n = 8; CTX R451C n = 8; one-way ANOVA  $^{*}P < .05$ .

### 3.5. Higher levels of ER molecular chaperones in the Purkinje cells from the R451C mice

Molecular chaperones of the ER are among the main target genes regulated by UPR (Rutkowski and Kaufman, 2007). The expression of ER markers in P60 adult cerebellar slices has been studied by co-immunolabeling of KDEL-containing ER proteins, which detects the ER chaperones BiP, Grp94 and PDI (Munro and Pelham, 1987), and the dendritic marker MAP2. R451C cerebellar slices showed consistent levels of KDEL staining in the soma of the PCs, which appeared stronger in intensity and different in distribution when compared to the staining observed in slices from WT mice (Fig. 7A). Quantification of the KDEL signal in PCs cells derived from the analysis of Z-stack images from either WT or R451C mice showed a higher KDEL intensity in the cerebellum of KI mice (Fig. 7B), indicating increased levels of ER chaperones, likely due to the activation of the UPR. In Fig. 7A, KDEL staining was also noticeable in the granule cell layer from R451C slices, containing the soma of the granule cells, which project to PCs. However, the small size of the soma and the high cellular density in this layer did not allow a reliable quantification of the signal.

Regarding the MAP-2 staining, as expected, this did not co-localize with KDEL and it is appreciable mainly in the dendritic branching. Bando and collaborators (Bando et al., 2012) previously showed NLGN3 immune reactivity in the molecular and granule layer and in the mossy fiber glomeruli in mouse cerebellar slices using a custom-made antibody. However, due to lack of good commercial antibodies for NLGN3 detection in immunohistochemistry, we were not able to reproduce these data.

## 4. Discussion

We have explored the role of the UPR in association to the ER retention of an ASDs-linked mutant protein. Previous studies have shown that mutations linked to ASDs in synaptic proteins such as NLGN3,

Caspr2 and CADM1, can lead to ER stress conditions, *in vitro*, and to activation of the UPR (Falivelli et al., 2012; Fujita et al., 2010; Ulbrich et al., 2016). Interestingly, a recent paper has reported altered ER stress gene expression in the brain of ASDs subjects (Cider et al., 2017). The R451C misfolding mutation in NLGN3 was shown to activate *in vitro* the ER stress sensors, ATF6, IRE1 and PERK, and to modulate the expression of UPR targets (Ulbrich et al., 2016). The UPR is a protective cellular pathway classically activated to ensure efficient protein folding capacity in the ER when the homeostasis of the organelle is challenged by altered physiological conditions, such as the over-load of misfolded proteins (Walter and Ron, 2011). Many human diseases are characterized by inherited or *de novo* mutations that lead to the accumulation of proteins in the ER, due to their failure to acquire a correct structural conformation during protein folding (De Jaco et al., 2012). Although compelling literature data support a role for UPR in the pathogenesis of several neurodegenerative diseases, where UPR signaling can eventually lead to neuronal death (Freeman and Mallucci, 2016; Hetz and Mollereau, 2014), few studies link UPR to neurodevelopmental disorders (Kawada and Mimori, 2017). However, a physiological role during brain development has been recently proposed for UPR in the regulation of neurogenesis, neuronal differentiation and cell fate specification (Godin et al., 2016; Murao and Nishitoh, 2017).

To the best of our knowledge, no studies have been published investigating the UPR in a mouse model for a monogenic form of ASDs, or the association between UPR and *in vivo* changes in synaptic transmission in specific brain areas implicated with ASDs. In this work, we have used the R451C NLGN3 KI mouse as a model system to study the cellular responses evoked by the endogenous R451C mutant protein in the brain. We confirmed that R451C NLGN3 is expressed in lower amount compared to WT protein, starting at early embryonic stages and up to E18. The reduced protein levels appear to be consequent to proteasome degradation, whereas the residual protein is partially retained in the ER, indicating that the misfolding induced by the R451C substitution affects protein stability, its exit from the ER and the proper

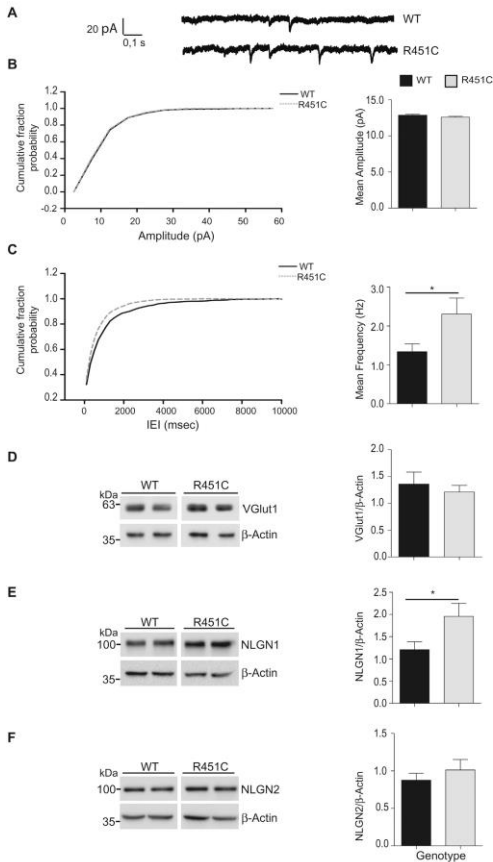


**Fig. 5.** Analysis of excitatory neurotransmission in the cerebellum of WT and R451C mice. **A.** Representative traces of mEPSCs recordings from WT and R451C mice. **B.** Cumulative amplitude distribution curves in cerebellar slices from WT and KI mice are identical. Bar-graph shows mean  $\pm$  SEM of the mEPSC amplitude recorded for the KI and WT mice (WT  $n = 19$  cells/9mice; R451C  $n = 19$  cells/9mice,  $P = .1504$ ; unpaired  $t$ -test). **C.** Cumulative distribution plots for the inter-event intervals (IEI) from WT and R451C mice showing a left shift for KI, indicating an increase of the mEPSC frequency (WT  $n = 19$ ; KI  $n = 19$ ,  $P = .0479$ ; unpaired  $t$ -test). **D.** Densitometric analysis and representative western blot of VGLUT1 levels normalized to  $\beta$ -Actin (mean  $\pm$  SEM; WT  $n = 4$ ; R451C  $n = 4$ ,  $P = .5828$ ; unpaired  $t$ -test). **E.** Densitometric analysis and representative western blot of NLGN1 levels normalized to  $\beta$ -Actin (mean  $\pm$  SEM; WT  $n = 12$ ; R451C  $n = 14$ ,  $P = .0463$ ; unpaired  $t$ -test). **F.** Densitometric analysis and representative western blot of NLGN2 levels normalized to  $\beta$ -Actin (mean  $\pm$  SEM; WT  $n = 8$ ; R451C  $n = 7$ ,  $P = .4183$ ; unpaired  $t$ -test).

localization of NLGN3 along the dendrites.

In the cerebellum of R451C NLGN3 mice, levels of the UPR marker BiP are increased at both embryonic and adult stages in comparison to WT. In this brain region, we also detected higher levels of phosphorylation of the UPR mediator eIF2 $\alpha$ , in comparison to WT. We show that reduction in the mutant NLGN3 levels is maintained in cerebellum,

hippocampus, and cerebral cortex, although UPR activation was not apparent in the two latter regions. Consistent with our findings, GCGs appear to be more sensitive to the UPR inducer tunicamycin than the cortical (Sun et al., 2013) and the hippocampal neurons (Kosuge et al., 2006). Moreover, the UPR has been reported to play an important role during the development of cerebellum and to be crucial for the survival

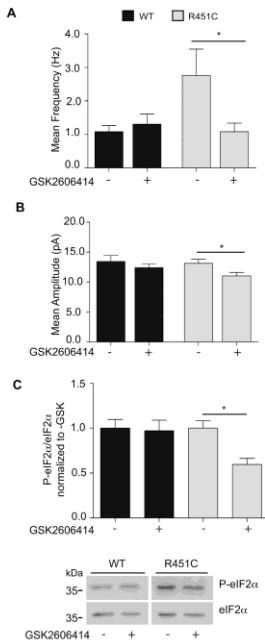


**Fig. 6.** Rescue of mEPSC frequency after inhibition of PERK in the R451C mice. **A.** Recording of the mEPSC amplitude in WT and R451C mice in control conditions or after treatment with GSK2606414. Statistical analysis compares GSK2606414-treated versus vehicle-treated control for each genotype. (mean  $\pm$  SEM; WT ctrl n = 11; WT treated n = 9,  $P = .4158$ ; R451C ctrl n = 10; R451C treated n = 12,  $P = .0304$ ; unpaired t-test). **B.** The bar-graph shows mEPSC frequency recorded with or without GSK2606414. Statistical analysis compares GSK2606414-treated versus vehicle-treated control for each genotype (mean  $\pm$  SEM; WT vehicle n = 6; WT treated n = 9,  $P = .5712$ ; R451C ctrl n = 10; R451C treated n = 12,  $P = .0410$ ; unpaired t-test). **C.** Densitometric analysis and representative western blot of P-eIF2 $\alpha$  normalized to total eIF2 $\alpha$  levels in lysates from WT and KI cerebellar slices with or without GSK2606414 treatment. Statistical analysis compares GSK2606414-treated versus vehicle-treated control for each genotype (mean  $\pm$  SEM; WT vehicle n = 4; WT GSK2606414 n = 3; R451C vehicle n = 5; R451C GSK2606414 n = 4; one-way ANOVA \* $P < .05$ ).

of PCs (Marzban et al., 2014). The higher sensitivity of these brain areas to ER stress could partially explain such a specific activation of UPR, although NLGN3 expression is ubiquitous in the brain (Varoqueaux et al., 2006).

Although alterations in excitatory synaptic transmission have been documented for R451C mice with differences at regional level between somatosensory cortex and hippocampus (Eherton et al., 2011a;

Pizzarelli and Cherubini, 2013; Tabuchi et al., 2007), functional properties in the cerebellum of the R451C mice have not been, thus far, investigated. Our data show altered excitatory neurotransmission on the PCs, which represent the main output of the cerebellum (Bassolino et al., 2012; Zhang and Südhof, 2016). Interestingly, we have correlated this phenotype with the activation of UPR by showing that the higher frequency of excitatory currents recorded in the PCs from R451C mice were rescued to WT levels after treatment with a specific inhibitor of PERK, indicating that the alteration in excitatory neurotransmission is due to the activation of this branch of the UPR. This finding is in line with previous evidences reporting the impact of ER stress on modulating the increase in spontaneous excitatory synaptic transmission in primary neuronal cultures (Nosyreva and Kavalali, 2010). The quantification of ER chaperone protein levels confirmed the up-regulation of UPR markers in PCs cells of cerebellar slices from R451C versus WT mice. We hypothesize that the activation of the UPR in the cerebellum involves not only the PCs but also the granule cell layer, since the parallel fibers from the CGCs represent the main excitatory input to PCs (Witter and De Zeeuw, 2015). A systematic analysis of the contribution of different NLGNs expressed in the cerebellum revealed that they differentially contribute to various PC synapses (Zhang et al., 2015). Here we show that in the cerebellum of the R451C NLGN3 KI mouse, NLGN1 and PSD95 levels are up-regulated in contrast to unchanged levels of NLGN2 and gephyrin. This further supports the potentiation of the excitatory glutamatergic transmission caused by the R451C mutation in this brain region, in comparison to WT mice. The higher probability of glutamate release from the CGCs parallel fibers does not seem to be due to a higher number of synapses, but rather to the UPR-induced changes in the release machinery in the presynaptic neuron. Neurotransmission impairment at parallel fibers-PCs synapses have been reported in the Shank2-deficient mice presenting ASDs-like behaviors, highlighting the involvement of the post-synaptic proteins on cerebellar function in the pathophysiology of ASDs (Peter et al., 2016).

Our data agree with recent studies on the role of the UPR in the regulation of synaptic function. The phosphorylation of eIF2 $\alpha$  has a critical role in the control of synaptic LTP and LTD in the hippocampus and in memory formation (Costa-Mattoli et al., 2007; Di Prisco et al., 2014), with PERK-dependent eIF2 $\alpha$  phosphorylation being required for mGluR-dependent LTD in the hippocampus (Trieh et al., 2014). The UPR mediator XBP1 has been hypothesized to modulate cognitive processes through the regulation of memory related genes such as BDNF, suggesting a possible regulation of brain functions through classical ER stress outputs (Hetz and Saxena, 2017; Martínez et al., 2016). Indeed, the R451C mouse has been shown to exhibit a phenotype characterized by enhanced spatial learning and LTP in hippocampus (Eherton et al., 2011a; Tabuchi et al., 2007) and impaired LTD in the dorsal striatum (Marella et al., 2017). Interestingly, UPR pathway has been shown to ensure the assembly and secretion of synaptic proteins in neurons, such as the export of the glutamate receptor from the ER, assembly and trafficking (Shim et al., 2004). Glutamate stimulation activates the IRE1 branch of UPR, the phosphorylation of eIF2 $\alpha$  and the up-regulation of BIP at post-synaptic sites in primary neurons, leading to the up-regulation of the BDNF (Saito et al., 2017).

Our data suggest that in the cerebellum of the R451C mice, activation of UPR caused by R451C NLGN3 retention in the ER triggers higher glutamate release, which could be due to either a cell-autonomous mechanism or a retrograde signal from the PCs to the presynaptic parallel fibers nerve terminal causing to release more vesicles. This mechanism could be then amplified by glutamate, by stimulating the activation of the UPR at the post-synaptic sites and creating a positive auto-regulatory loop between the PCs and the granule cells. Activation of UPR signaling in the cerebellum of this mouse model could lead to neuronal circuits alterations and play a role in the autistic phenotype by impacting the cerebellar outputs to the sensorimotor and cognitive regions of the cerebral cortex and to the multi-synaptic connections of the hippocampus (D'Mello and Stoodley, 2015; Rochefort et al., 2013). This

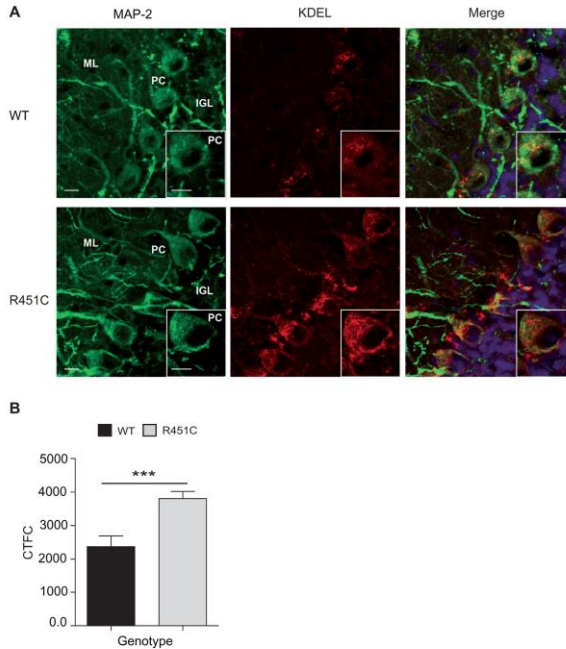


**Fig. 7.** Immunostaining for KDEL and MAP2 on cerebellar slices. **A.** Immunofluorescence detection of KDEL in cerebellar slices from R451C and WT mice. KDEL (red) in the Purkinje cells (PC), in the internal granule layer (IGL) and in the molecular layer (ML). An antibody against MAP2 (green) was used as neuronal marker. Draq5 was used to stain the nuclei (40× magnification, 1.9× zoom). Scale bar corresponds to 10 μm. **B.** The bar-graph shows semi-quantitative analysis of the corrected total cell fluorescence (CTFC) intensity for KDEL staining in the cerebellar Purkinje cells of WT and R451C adult mice (mean ± SEM; WT n = 38 cells/12 z-stack images from 3 mice; R451C n = 53 cells/ 14 z-stack images from 3 mice,  $P = .0002$ ; unpaired t-test). (For interpretation of the references to colour in this figure legend, the reader is referred to the web version of this article.)

extensive connectivity provides an anatomical substrate by which cerebellar dysfunctions could be involved in the large spectrum of symptoms characterizing ASDs (Rogers et al., 2013; Wang et al., 2014).

In conclusion, we show here that the ASDs-linked R451C misfolding mutation in NLGN3 activates the UPR *in vivo*, specifically in the cerebellum, leading to synaptic transmission alterations in the Purkinje cells.

Supplementary data to this article can be found online at <https://doi.org/10.1016/j.nbd.2018.08.026>.

#### Declaration of interest

The authors declare that they have no conflicts of interest with the contents of this article.

#### Funding sources

This work was supported by: Compagnia San Paolo, Sapienza research grant 2016 and Italian Pasteur Institute - Cenci Bolognietti Foundation grants to ADJ. This work was also supported by the Governor's Council for Medical Research and Treatment of Autism [CAUT14APL028] and from the Robert Wood Johnson Foundation to the Child Health Institute of New Jersey [grant #74260] to D.C. Funding to CL were from Sapienza University of Rome 2017, PRIN 2015 and Italian Ministry of Health. EM was supported by Sapienza research grants and Italian Pasteur Institute - Cenci Bolognietti Foundation.

#### Acknowledgements

We thank Silvana Caristi for assistance with the use of the confocal

microscope, Andrea Setini and Vince Mirabella for discussion and Andrea Barberis for providing the mating couple to originate the mouse colony.

## References

- Abrahams, B.S., Geschwind, D.H., 2008. Advances in genetic genetics on the threshold of a new neurobiology. *Nat. Rev. Genet.* 9, 341–355. <https://doi.org/10.1038/nrn2346>.
- Annes, V., Herrero, M.-T., Di Pentima, M., Gomez, A., Lombardi, L., Ros, C.M., De Pablo, V., Hernandez-Villasca, E., De Stefano, M.E., 2015. Metalloproteinase-9 contributes to inflammatory glia activation and nigro-striatal pathway degeneration in both mouse and monkey models of 1-methyl-4-phenyl-1,2,3,6-tetrahydropyridine (MPTP)-induced Parkinsonism. *Brain Struct. Funct.* 220, 770–777. <https://doi.org/10.1007/s00429-014-0718-8>.
- Baig, D.N., Yanagawa, T., Tabuchi, K., 2017. Distortion of the normal function of synaptic cell adhesion molecules by genetic variants as a risk for autism spectrum disorders. *Brain Res. Bull.* 129, 82–90. <https://doi.org/10.1016/j.brainresbull.2016.10.006>.
- Baudouin, S.J., Caudais, J., Gerbazi, S., Hasnott, L., Zhou, K., Punamäke, P., Tanaka, K.F., Spooner, W., Hen, R., De Zeeuw, C.J., Vogt, K., Scheiffele, P., 2012. Shared synaptic pathology in syndromic and non-syndromic rodent models of autism. *Science* 338, 128–132. <https://doi.org/10.1126/science.1224189>.
- Bourgeron, T., 2009. A synaptic tract in autism. *Curr. Opin. Neurobiol.* 19, 231–234. <https://doi.org/10.1016/j.con.2009.06.003>.
- Bourgeron, T., 2015. From the genetic architecture to synaptic plasticity in autism spectrum disorder. *Nat. Rev. Neurosci.* 16, 591–593. <https://doi.org/10.1038/nrn3992>.
- Budreck, E.C., Scheiffele, P., 2007. Neuroligin-3 is a neuronal adhesion protein at GABAergic and glutamatergic synapses. *Dev. J. Neurosci.* 26, 1738–1748. <https://doi.org/10.1111/j.1460-9568.2007.05842.x>.
- Camp, S., Zhang, L., Krejci, E., Dobbertin, A., Bernard, V., Girard, E., Duxsen, E.G., Lockridge, O., De Jaco, A., Taylor, P., 2010. Contributions of selective knockout studies to understanding cholineesterase disposition and function. *Chem. Biol.* 18, 777–779. <https://doi.org/10.1016/j.cub.2010.02.008>.
- Cantieri, S., Bosco, A., Carletti, V., Fusco, A., Carci, A., Mangia, F., Fiorenza, M.T., 2012. Subcellular TSC2/4 localization in cerebellum granule neurons of the mouse depends on development and differentiation. *Cerebellum* 11, 28–40. <https://doi.org/10.1007/s12311-010-0211-8>.
- Celler, G., Cherubini, E., 2014. Reduced inhibitory gate in the barrel cortex of Neuroligin3/RASIC knock-in mice: an animal model of autism spectrum disorders. *Physiol. Rep.* 2. <https://doi.org/10.1151/phys.2014.210277>.
- Chambers, J.L., Marciniak, S.J., 2014. Cellular mechanisms of endoplasmic reticulum stress signaling in health and disease. 2. Protein misfolding and ER stress. *Am. J. Physiol. Cell Physiol.* 307, C657–C670. <https://doi.org/10.1152/ajpcell.00183.2014>.
- Chih, B., Afridi, S.K., Clark, L., Scheiffele, P., 2004. Disorder-associated mutations lead to functional inactivation of neuroligins. *Hum. Mol. Genet.* 13, 1471–1477. <https://doi.org/10.1093/hmg/ddh158>.
- Comolletti, D., De Jaco, A., Jennings, L.L., Flynn, R.E., Galetta, G., Tsigelny, L., Ellisman, M.H., Taylor, P., 2004. The Arg551Cys-neuroligin-3 mutation associated with autism reveals a defect in protein processing. *J. Neurosci.* 24, 4889–4893. <https://doi.org/10.1523/JNEUROSCI.1468-04.2004>.
- Costa-Mattoli, M., Gobert, D., Stern, E., Gamache, C., Collina, R., Cuello, C., Sossin, W., Kaufman, R., Pelletier, J., Rosenblum, K., Krnjević, K., Lacaille, J.-C., Nader, K., Sonenberg, N., 2007. eIF2alpha phosphorylation bidirectionally regulates the switch from short- to long-term synaptic plasticity and memory. *Cell* 129, 195–206. <https://doi.org/10.1016/j.cell.2007.01.050>.
- Czider, A., Ahmed, A.O., Pillai, A., 2017. Altered expression of endoplasmic reticulum stress-related genes in the middle frontal cortex of subjects with autism spectrum disorder. *Mol. Neuropsychiatry* 3, 85–91. <https://doi.org/10.1159/000477212>.
- De Jaco, A., Comolletti, D., Kovarik, Z., Galetta, G., Radic, Z., Lockridge, O., Ellisman, M.H., Taylor, P., 2006. A mutation linked with autism reveals a common mechanism of endoplasmic reticulum retention for the alpha-beta-hydrolase fold protein family. *J. Biol. Chem.* 281, 9667–9676. <https://doi.org/10.1074/jbc.M510262000>.
- De Jaco, A., Comolletti, D., King, C.G., Taylor, P., 2008. Trafficking of cholineesterases and neuroligin mutant proteins: An association with autism. *Chem. Biol. Interact.* 175, 349–351. <https://doi.org/10.1016/j.cbi.2008.04.023>.
- De Jaco, A., Dabi, N., Comolletti, D., Taylor, P., 2010a. Folding anomalies of neuroligin-3 caused by a mutation in the alpha-beta-hydrolase fold domain. *Chem. Biol. Interact.* 187, 56–58. <https://doi.org/10.1016/j.cbi.2010.05.012>.
- De Jaco, A., Lin, M.Z., Dabi, N., Comolletti, D., Miller, M.T., Camp, S., Ellisman, M., Butko, M.T., Tsien, R.Y., Taylor, P., 2010b. Neuroligin trafficking deficiencies arising from mutations in the alpha-beta-hydrolase fold protein family. *J. Biol. Chem.* 285, 28674–28682. <https://doi.org/10.1074/jbc.M110.139519>.
- De Jaco, A., Comolletti, D., Dabi, N., Camp, S., Taylor, P., 2012. Processing of choline-esterase-like alpha-beta-hydrolase fold proteins: alterations associated with congenital disorders. *Trends Pept. Lett.* 19, 173–179.
- De Rubis, S., He, X., Goldberg, A.P., Poulney, C.S., Samocha, K., Cleck, A.E., Kou, Y., Liu, L., Fromer, M., Walker, S., Singh, T., Klei, L., Komaki, J., Shih-Chen, F., Alekic, B., Biscaldi, M., Bolger, P.F., Brownfield, J.M., Cai, J., Campbell, N.G., Carracedo, A., Chahour, M.H., Chiochetti, A.G., Coon, H., Crawford, E.L., Curran, S.R., Dawson, G., Dukatis, E., Fernandez, B.A., Gallagher, A., Geller, E., Guter, S.J., Hill, R.S., Imitola, J., Jimenez-Gonzalez, P., Kilpinen, H., Klauk, M.S., Kolevzon, A., Lee, L., Lei, L., Lei, L., Lehtmäki, T., Lin, C.-F., Marjan, A., Marshall, C.R., McKusick, A.J., Neale, B., Owen, M.J., Ozaki, N., Paré, M., Parr, J.R., Purcell, S., Putra, K., Rajagopalan, D., Rehrström, K., Reichenberger, A., Sabo, A., Sachs, M., Sanders, S.J., Schaefer, C.,

- Schüle-Rüther, M., Skuse, D., Stevens, C., Stattner, P., Tannirries, K., Valladares, O., Viana, A., Li-San, W., Weiss, L.A., Willsey, A.J., Yu, T.-F., Yuen, R.K.C., DED Study, Homozygosity Mapping Collaborative for Autism, UK10K Consortium, Cook, E.H., Freitag, C.M., Gill, M., Hultman, C.M., Lehner, T., Palotie, A., Schellenberg, G.D., Sklar, P., State, M.W., Sutcliffe, J.S., Walsh, C.A., Scherer, S.W., Zwick, M.E., Barrett, J.C., Cutler, D.J., Roeder, K., Devita, B., Daly, M.J., Buckman, J.D., 2014. Synaptic, transcriptional and chromatin genes disrupted in autism. *Nature* 515, 209–215. <https://doi.org/10.1038/nature13772>.
- D'Arcos, G.V., Huang, W., Buffington, S.A., Han, C.-C., Boman, P.E., Placzek, A.L., Sidranski, C., Krnjević, K., Kaufman, R.J., Walter, P., Costa-Mattoli, M., 2014. Translational control of mGluR-dependent long-term depression and object-place learning by eIF2a. *Nat. Neurosci.* 17, 1073–1082. <https://doi.org/10.1038/nn.3754>.
- D'Amico, A.M., Stoodley, C.J., 2015. Cerebro-cerebellar circuits in autism spectrum disorder. *Front. Neurosci.* 9 (408). <https://doi.org/10.3389/fnins.2015.00408>.
- Eberhart, M., Földy, C., Sharma, M., Tabuchi, K., Liu, X., Shamloo, M., Malenka, R.C., Südhof, T.C., 2011a. Autism-linked neuroligin-3 R451C mutation differentially alters hippocampal and cortical synaptic function. *Proc. Natl. Acad. Sci. U. S. A.* 108, 13764–13769. <https://doi.org/10.1073/pnas.111093108>.
- Eberhart, M.R., Tabuchi, K., Sharma, M., Ko, J., Südhof, T.C., 2011b. An autism-associated point mutation in the neuroligin cytoplasmic tail selectively impairs AMPA receptor-mediated synaptic transmission in hippocampus. *EMBO J.* 30, 2908–2919. <https://doi.org/10.1038/emboj.2011.182>.
- Falvelli, G., De Jaco, A., Favaloro, E.L., Kim, H., Wilson, J., Dabi, N., Ellisman, M.H., Abrahams, B.S., Taylor, P., Comolletti, D., 2012. Inherited genetic variants in autism-related CNTNAP2 show perturbed trafficking and AT76 activation. *Hum. Mol. Genet.* 21, 4761–4773. <https://doi.org/10.1093/hmg/ddq320>.
- Földy, C., Malenka, R.C., Südhof, T.C., 2013. Autism-associated neuroligin-3 mutations commonly disrupt tonic endocannabinoid signaling. *Neuron* 78, 498–509. <https://doi.org/10.1016/j.neuron.2013.02.026>.
- Freeman, O.J., Mallucci, G.R., 2016. The UPF and synaptic dysfunction in neurodegeneration. *Brain Res.* 1648, 530–537. <https://doi.org/10.1016/j.brainres.2016.03.029>.
- Fujita, E., Dai, H., Tanahe, Y., Zhiling, Y., Yamagata, T., Miyakawa, T., Tanokura, M., Momoi, M.Y., Momoi, T., 2010. Autism spectrum disorder is related to endoplasmic reticulum stress induced by mutations in the synaptic cell adhesion molecule, CADM1. *Cell Death Dis.* 1, e47. <https://doi.org/10.1038/cddis.2010.23>.
- Godin, J.J., Creppe, C., Laguesse, S., Nguyen, L., 2016. Emerging roles for the unfolded protein response in the developing nervous system. *Trends Neurosci.* 39, 394–404. <https://doi.org/10.1016/j.tins.2016.04.002>.
- Hetz, C., Molleurau, B., 2014. Disturbance of endoplasmic reticulum proteostasis in neurodegenerative diseases. *Nat. Rev. Neurosci.* 15, 233–249. <https://doi.org/10.1038/nrn3689>.
- Hetz, C., Saxena, S., 2017. ER stress and the unfolded protein response in neurodegeneration. *Nat. Rev. Neurosci.* 13, 477–491. <https://doi.org/10.1038/nrn2017.99>.
- Hetz, C., Chevet, E., Harding, H.P., 2013. Targeting the unfolded protein response in disease. *Nat. Rev. Drug Discov.* 12, 703–719. <https://doi.org/10.1038/nrn3976>.
- Hoon, M., Soykan, T., Falkenburger, B., Hammer, M., Patrizi, A., Schmidt, K.F., Sasso-Pognetto, M., Löwel, S., Moser, T., Taschenberger, H., Brose, N., Varoqueaux, F., 2011. Neuroligin-4 is localized to glycinergic postsynapses and regulates inhibition in the retina. *Proc. Natl. Acad. Sci. U. S. A.* 108, 3053–3058. <https://doi.org/10.1073/pnas.1006946108>.
- Iwawaki, T., Akai, R., Kohno, K., Miura, M., 2004. A transgenic mouse model for monitoring endoplasmic reticulum stress. *Nat. Med.* 10, 98–102. <https://doi.org/10.1038/nm970>.
- Jamain, S., Quach, H., Betancur, C., Råstam, M., Colineaux, C., Gillberg, I.C., Söderstrom, H., Gires, B., Leboyer, M., Gillberg, C., Bourgeron, T., Paris Autism Research International Sibipair Study, 2003. Mutations of the X-linked genes encoding neuroligins NLGN3 and NLGN4 are associated with autism. *Cell* 114, 27–29. <https://doi.org/10.1038/ng1136>.
- Jamain, S., Radyushkin, K., Hammerschmidt, K., Granon, S., Boretius, S., Varoqueaux, F., Rammannston, N., Gallegos, J., Ronneberg, A., Winter, D., Frahm, J., Fischer, J., Bourgeron, T., Ehrlich, H., Brose, N., 2008. Reduced social interaction and ultrasonic communication in a mouse model of monogenic heritable autism. *Proc. Natl. Acad. Sci. U. S. A.* 105, 1710–1715. <https://doi.org/10.1073/pnas.0713551105>.
- Kawada, K., Minori, S., 2017. Implication of endoplasmic reticulum stress in autism spectrum disorder. *Neurochem. Res.* 42, 285–293. <https://doi.org/10.1007/s12064-017-2370-1>.
- Kouge, Y., Sakaiuchi, T., Ishige, K., Ito, Y., 2006. Comparative study of endoplasmic reticulum stress-induced neuronal death in rat cultured hippocampal and cerebellar granule neurons. *Neurochem. Int.* 49, 285–293. <https://doi.org/10.1016/j.neuint.2006.01.021>.
- de la Torre-Ucar, L., Won, H., Stein, J.L., Geschwind, D.H., 2016. Advancing the understanding of autism disease mechanisms through genetics. *Nat. Med.* 22, 345–361. <https://doi.org/10.1038/nm.4071>.
- Lee, E., Lee, J., Kim, E., 2016. Excitation/inhibition imbalance in animal models of autism spectrum disorders. *Biol. Psychiatry.* 2016. <https://doi.org/10.1016/j.biopsych.2016.05.011>.
- Livak, K.J., Schmittgen, T.D., 2001. Analysis of relative gene expression data using real-time quantitative PCR and the 2<sup>-ΔΔCT</sup> method. *Methods* 25, 402–408. <https://doi.org/10.1006/meth.2001.1322>.
- Maheshwari, R.K., Husain, M.M., Attallah, A.M., Friedman, R.M., 1983. Tunicamycin treatment inhibits the antiviral activity of interferon in mice. *FEBS Lett.* 161, 61–66.
- Martella, G., Meringolo, M., Trobiano, L., De Jaco, A., Pisani, A., Bonisi, P., 2017. The neurobiological bases of autism spectrum disorders: the R451C-neuroligin-3 mutation hampers the expression of long-term depression in the dorsal striatum. *Dev. J. Neurosci.* 2017. <https://doi.org/10.1111/djn.13705>.
- Martinez, G., Vidal, R.L., Mardones, P., Serrano, F.G., Ardiles, A.O., Wirth, C., Valdés, P.,

- Thielen, P., Schneider, B.L., Kerr, B., Valdeís, J.J., Palacios, A.G., Inestrosa, N.C., Glücher, L.H., Hietz, C., 2016. Regulation of Memory Formation by the Transcription Factor XBP1. *Cell Rep.* **14**, 1382–1394. <https://doi.org/10.1016/j.celrep.2016.01.028>.
- Márzban, H., Del Bigio, M.R., Alizadeh, J., Ghavami, S., Zecharahn, R.M., Rastegar, M., 2014. Cellular commitment in the developing cerebellum. *Front. Cell. Neurosci.* **8**, 450. <https://doi.org/10.3389/fncel.2014.00450>.
- Munro, S., Pelham, H.R., 1987. A C-terminal signal prevents secretion of luminal ER proteins. *Cell* **48**, 899–907.
- Murao, N., Nishitoh, H., 2017. Role of the unfolded protein response in the development of central nervous system. *J. Biochem. (Tokyo)* **162**, 155–162. <https://doi.org/10.1093/jb/mvz047>.
- Nakanishi, M., Nomura, J., Ji, X., Tamada, K., Arai, T., Takahashi, E., Bucan, M., Takumi, T., 2017. Functional significance of rare neurotulin-1 variants found in autism. *PLoS Genet.* **13**, e1006940. <https://doi.org/10.1371/journal.pgen.1006940>.
- Nosyreva, E., Kavali, E.T., 2010. Activity-dependent augmentation of spontaneous neurotransmission during endoplasmic reticulum stress. *J. Neurosci.* **30**, 7358–7368. <https://doi.org/10.1523/JNEUROSCI.5358-09.2010>.
- Palladino, G., Loizzo, S., Fortuna, A., Canterini, S., Palombi, F., Erickson, R.P., Mangia, F., Fiorina, M.T., 2015. Visual evoked potentials of Niemann-Pick type C1 mice reveal an impairment of the visual pathway that is rescued by 2-hydroxypropyl- $\beta$ -cyclodextrin. *Orphanet J. Rare Dis.* **10** (133). <https://doi.org/10.1186/s13023-015-0348-4>.
- Peter, S., Ten Brink, M.M., Stedehouder, J., Reinel, C.M., Wu, B., Zhou, H., Zhou, K., Boede, H.-J., Kuschner, S.A., Lee, M.G., Schmeisser, M.J., Boeckers, T.M., Schoneweille, M., Hoebbeck, F.E., De Zeeuw, C.I., 2016. Dysfunctional cerebellar Purkinje cells contribute to autism-like behaviour in Shank2-deficient mice. *Nat. Commun.* **7**, 12627. <https://doi.org/10.1038/ncomms12627>.
- Pizzarelli, R., Cherabini, E., 2013. Developmental regulation of GABAergic signalling in the hippocampus of neurotulin-3 R451C knock-in mice: an animal model of Autism. *Front. Cell. Neurosci.* **7** (83). <https://doi.org/10.3389/fncel.2013.00085>.
- Radyushkin, K., Hammerschmidt, K., Boretius, S., Varoqueaux, F., El-Kordi, A., Rommenga, A., Witter, D., Frhm, J., Fischer, J., Brose, N., Ehrenreich, H., 2009. Neurotulin-3-deficient mice: model of a monogenic heritable form of autism with an olfactory deficit. *Genes Brain Behav.* **8**, 416–425. <https://doi.org/10.1111/j.1601-183X.2009.00487.x>.
- Rochefort, C., Lefort, J.M., Rondi-Reig, L., 2013. The cerebellum: a new key structure in the navigation system. *Front. Neural Circuits* **7** (83). <https://doi.org/10.3389/fncir.2013.00035>.
- Rogers, T.D., Dickson, P.E., McKim, E., Heck, D.H., Goldowitz, D., Blaha, C.D., Mittleman, G., 2013. Reorganization of circuits underlying cerebellar modulation of prefrontal cortical dopamine in mouse models of autism spectrum disorder. *Cerebellum Lond. Engl.* **12**, 547–556. <https://doi.org/10.1007/s12311-013-0462-2>.
- Roussel, B.D., Krappas, A.J., Miranda, E., Crowther, D.G., Lomas, D.A., Marciniak, S.J., 2013. Endoplasmic reticulum dysfunction in neurological disease. *Lancet Neurol.* **12**, 105–118. [https://doi.org/10.1016/S1474-4422\(12\)70288-7](https://doi.org/10.1016/S1474-4422(12)70288-7).
- Rutkowski, D.T., Kaufman, R.J., 2007. That which does not kill me makes me stronger: adapting to chronic ER stress. *Trends Biochem. Sci.* **32**, 469–476. <https://doi.org/10.1016/j.tics.2007.09.003>.
- Saito, A., Cai, L., Matsushita, K., Ohtake, Y., Kaneko, M., Kanemoto, S., Asada, R., Imazumi, K., 2017. Neuronal activity-dependent local activation of dendritic unfolded protein response promotes expression of brain-derived neurotrophic factor in cell soma. *J. Neurochem.* <https://doi.org/10.1111/jnc.14221>.
- Shim, J., Umemura, T., Notstein, E., Rongo, C., 2004. The unfolded protein response regulates glutamate receptor export from the endoplasmic reticulum. *Mol. Biol. Cell* **15**, 4814–4828. <https://doi.org/10.1091/jmb.104.42.4818>.
- Song, J.Y., Ichtchenko, K., Südhof, T.C., Brose, N., 1999. Neurotulin-1 is a postsynaptic cell-adhesion molecule of excitatory synapses. *Proc. Natl. Acad. Sci. U. S. A.* **96**, 1100–1105.
- Südhof, T.C., 2008. Neurotulin and neuroligin link synaptic function to cognitive disease. *Nature* **455**, 903–911. <https://doi.org/10.1038/nature07456>.
- Sun, L., Zhao, Y., Zhou, K., Freeze, H.H., Zhang, Y.-W., Xu, H., 2013. Insufficient ER stress response causes selective mouse cerebellar granule cell degeneration resembling that seen in congenital disorders of glycosylation. *Mol. Brain* **6**, 52. <https://doi.org/10.1186/1756-6606-6-52>.
- Sun, Y., Iran, T., Davis, M.F., Gong, N., Zheng, K., Luo, Z.D., Lai, C., Mei, L., Holmes, T.C., Gandhi, S.P., Xu, X., 2016. Neurotulin-1/Erh4 Signaling Regulates Visual Cortical Plasticity. *Neuron* **92**, 160–173. <https://doi.org/10.1016/j.neuron.2016.08.033>.
- Tabuchi, K., Blumfeld, J., Eberton, M.R., Hammer, R.E., Liu, X., Powell, C.M., Südhof, T.C., 2007. A neurotulin-3 mutation implicated in autism increases inhibitory synaptic transmission in mice. *Science* **318**, 71–76. <https://doi.org/10.1126/science.1146221>.
- Takayangi, S., Fukuda, R., Takeuchi, Y., Takeda, S., Yoshida, K., 2013. Gene regulatory network of unfolded protein response genes in endoplasmic reticulum stress. *Cell Stress Chaperones* **18**, 11–23. <https://doi.org/10.1007/s12192-012-0351-5>.
- Talebizadeh, Z., Lam, D.Y., Theodore, M.F., Bittel, D.C., Lushington, G.H., Butler, M.G., 2008. Novel splice isoforms for NLGN3 and NLGN4 with possible implications in autism. *J. Med. Genet.* **45**, e21. <https://doi.org/10.1136/jmg.2005.036897>.
- Trinh, M.A., Ma, T., Kaphzan, H., Bhattacharya, A., Anton, M.D., Caveney, D.R., Hoeffler, C.A., Klann, E., 2014. The eIF2a kinase PERK limits the expansion of hippocampal metabotropic glutamate receptor-dependent long-term depression. *Learn. Mem.* *Gold Spring Harb.* **21**, 298–304. <https://doi.org/10.1101/m.032219.113>.
- Ulbrich, L., Favalaro, F.L., Trobiansi, L., Marchetti, V., Patel, V., Pascucci, T., Comolletti, D., Marciniak, S.J., De Jaco, A., 2016. Autism-associated R551C mutation in neurotulin-3 leads to activation of the unfolded protein response in a PC12 Tet-On inducible system. *Biochem. J.* **473**, 423–434. <https://doi.org/10.1042/bj20150274>.
- Varoqueaux, F., Jamin, S., Brose, N., 2004. Neurotulin-2 is exclusively localized to inhibitory synapses. *Eur. J. Cell Biol.* **83**, 449–456. <https://doi.org/10.1078/s0071-9335-04010>.
- Varoqueaux, F., Aramini, G., Rawson, R.L., Mohrman, R., Misdler, M., Gottmann, K., Zhang, W., Südhof, T.C., Brose, N., 2006. Neurotulin-deficient synapse maturation and function. *Neuron* **51**, 741–754. <https://doi.org/10.1016/j.neuron.2006.09.003>.
- Walter, P., Ron, D., 2011. The unfolded protein response: from stress pathway to homeostatic regulation. *Science* **334**, 1081–1086. <https://doi.org/10.1126/science.1209008>.
- Wang, S.S.-H., Kloth, A.D., Badura, A., 2014. The cerebellum, sensitive periods, and autism. *Neuron* **83**, 518–532. <https://doi.org/10.1016/j.neuron.2014.07.016>.
- Wang, X., Kery, R., Xiong, Q., 2017. Synaptopathology in autism spectrum disorders: Complex effects of synaptic genes on neural circuits. *Prog. Neuro Psychopharmacol. Biol. Psychiatry.* <https://doi.org/10.1016/j.pnpb.2017.09.026>.
- Witter, L., De Zeeuw, C.I., 2015. Regional functionality of the cerebellum. *Curr. Opin. Neurobiol.* **33**, 150–155. <https://doi.org/10.1016/j.conb.2015.03.017>.
- Yan, S., Wang, C.-E., Wei, W., Gaertig, M.A., Lai, L., Li, S., Li, X.-J., 2014. TDP-43 causes differential pathology in neuronal versus glial cells in the mouse brain. *Hum. Mol. Genet.* **23**, 2678–2693. <https://doi.org/10.1093/hmg/ddt662>.
- Zhang, B., Südhof, T.C., 2016. Neurotulin is selectively essential for NMDAR signaling in cerebellar stellate interneurons. *J. Neurosci.* **36**, 9079–9083. <https://doi.org/10.1523/JNEUROSCI.1356-16.2016>.
- Zhang, C., Milinsky, J.M., Newton, S., Jin, J., Zhao, G., Maher, T.A., Tager-Flusberg, G. H., Bolliger, M.F., Carter, A.S., Boucard, A.A., Powell, C.M., Südhof, T.C., 2009. A neurotulin-4 missense mutation associated with autism impairs neurotulin-4 folding and endoplasmic reticulum export. *J. Neurosci.* **29**, 10843–10854. <https://doi.org/10.1523/JNEUROSCI.1248-09.2009>.
- Zhang, B., Chen, L.Y., Liu, X., Maxeiner, S., Lee, S.-J., Gokce, O., Südhof, T.C., 2015. Neurotulin sculpt cerebellar purkinje-cell circuits by differential control of distinct classes of synapses. *Neuron* **87**, 781–796. <https://doi.org/10.1016/j.neuron.2015.07.020>.
- Zimmermann, H.R., Yang, W., Beckelman, B.C., Kasica, N.P., Zhou, X., Galli, L., Ryzanov, A.G., Ma, T., 2018. Genetic Removal of eIF2a Kinase PERK in Mice Enables Hippocampal LTP Independent of mTORC1 Activity. *J. Neurochem.* <https://doi.org/10.1111/jnc.14306>.

## **CHAPTER II:**

### **Screening of chemical compounds to restore the defective trafficking of R451C Neuroigin3**

#### **Introduction**

The Endoplasmic Reticulum (ER) is the cellular compartment responsible for the synthesis of one-third of the proteome, through the action of ER-resident chaperones (Halperin et al., 2014). Furthermore, several post-translational modifications take place in the ER, mostly represented by glycosylation and disulfide bond formation (Takayanagi et al., 2013). The folding and glycosylation state of proteins is monitored by the quality control system of the organelle, which allows only proteins correctly folded to undertake the secretory pathway; than otherwise would be shuttled for the ER-mediated degradation (ERAD) (Corazzari et al., 2017; Hebert and Molinari, 2007).

To ensure these functions, the ER requires a fine homeostatic state to avoid perturbations that can lead to ER stress conditions. In case of stress, a highly conserved signaling pathway, the Unfolded Protein Response (UPR) is activated with the aim of restoring ER homeostasis by attenuating protein synthesis, enhancing protein folding capacity of the ER and protein degradation through the ERAD (Chambers and Marciniak, 2014).

The accumulation of misfolded/unfolded proteins and UPR activation are hallmarks of several neurological and non-neurological diseases, collectively called protein misfolding

disorders, such as Alzheimer's, Parkinson's, diabetes and cancer (Mercado et al., 2016; Corazzari et al., 2017).

Recently, a growing interest is focused on developing small-molecule drugs with chaperone-like activity, able to restore protein folding, by reducing the accumulation of misfolded proteins and re-establish normal trafficking to the appropriate subcellular localization.

Numerous pharmacological and chemical chaperones have been tested both *in vitro* and *in vivo* in disease model systems and some of them reached the stage of clinical trials (Cortez and Sim, 2014). The well-known chemical chaperones, sodium 4-phenylbutyrate (4-PBA) and Trimethylamine N-oxide dihydrate (TUDCA), have been shown to reduce ER stress in a mouse model of type II diabetes by increasing folding capacity (Ozcan et al., 2006). 4-PBA has also been tested *in vivo*, in mouse models of cerebral ischemic injury and spinal cord ischemia, showing positive effects on reducing ER stress and alleviating neurological damages (Qi et al., 2004; Mizukami et al., 2010). Among the neurological disorders, in the last years, several cellular pathways have been characterized for underlying Autism Spectrum Disorders (ASDs). Mutations in genes encoding for synaptic proteins have been studied at the molecular level for possible folding and trafficking impairments. Among these, the synaptic family of Neuroligins (NLGNs) proteins represent a group of proteins well-characterized (de la Torre-Ubieta et al., 2016; Baig et al., 2017). NLGNs are post-synaptic cell-adhesion molecules, playing a role in synaptic organization and function, through the interaction with the pre-synaptic family of proteins Neurexins (NRXNs) and with scaffolding proteins (Südhof 2008, 2017).

*NLGN3* and *NLGN4* were initially considered the most interested by ASDs-associated mutations. However, several mutations have been recently found in the *NLGN1* gene (Nakanishi et al., 2017)

It is noteworthy that most of these mutations impact on the folding of the protein extracellular domain, occurring in the ER, resulting in reduced trafficking of the mutant protein to the cell surface. The lack of these proteins at their proper localization, affect synaptic functions and cause behavioral defects (Ribeiro et al., 2018).

Among the NLGNs mutations, the most studied is the substitution Arg451Cys (R451C) in *NLGN3*, which causes a local misfolding of the extracellular protein domain (De Jaco et al., 2010). The extent of the misfolding is sufficient to cause the retention of the mutant *NLGN3* in the ER, leading to the activation of the UPR in PC12 Tet-on cell lines with inducible expression of *NLGN3* (De Jaco et al., 2006; Ulbrich et al., 2016).

The Knock-In (KI) mouse carrying the R451C mutation in the endogenous *NLGN3* gene, represents a model of a monogenic form of ASDs for its autistic-like behaviors and imbalance in the excitatory/inhibitory neurotransmission ratio (Tabuchi et al., 2007; Etherton et al., 2011). We have shown a drastic reduction in mutant *NLGN3* protein levels in the whole brain during development and in the adulthood, supporting the effect of the mutation on protein stability *in vivo* (Trobiani et al., 2018). The mutant protein is also retained in the ER in the whole brain of the R451C KI mouse and UPR is selectively activated in the cerebellum, where it modulates neurotransmission (Trobiani et al., 2018).

In this work, we aimed at generating an easy-to-use model system for the screening of chemical compounds with chaperone-like activity acting at improving protein folding in the ER in order to favor the escape of the mutant NLGN3 from the organelle, restoring its physiological expression to the cell surface and alleviating UPR.

This would represent a possible strategy to treat the monogenic form of ASDs caused by the R451C mutation in NLGN3, but it would be potentially useful for other protein misfolding diseases due to the retention of mutant proteins in the ER.

## **Results**

### **Generation of HEK293 cell lines expressing truncated and fluorescent NLGN3**

Previous studies showed alterations of the full-length R451C NLGN3 protein trafficking through the secretory pathway. Indeed, the mutant protein was shown to be retained in the ER failing to reach the cell surface (De Jaco et al., 2006, 2010). We have generated a new cell-based model system to study NLGN3 trafficking by using HEK293 cell lines stably expressing a truncated form of NLGN3 made of the extracellular protein domain, lacking the transmembrane and intracellular protein domains, and C-terminally fused to the Venus Fluorescent Protein (Giepmans et al., 2006) (Fig. 1A). These cell lines produce a fluorescent NLGN3, either WT or R451C, that is secreted by the cell, allowing to evaluate protein trafficking by measuring fluorescence levels in the cell culture medium. We have generated several clones expressing the truncated protein forms that were characterized for the levels of fluorescence in the medium and the levels of protein expression (Fig. 1B).

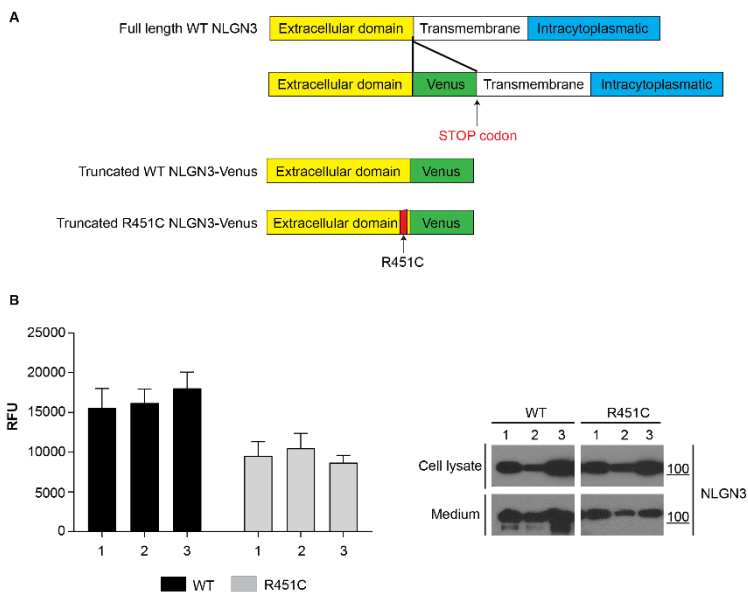


## Figure 1. Generation of HEK293 cell lines expressing truncated and fluorescent NLGN3

A. Schematic representation of the vectors encoding for the NLGN3 truncated and fluorescent protein forms.

B. Fluorescence levels (RFU) and representative western blot of cell medium and lysates from three stably transfected clones (mean  $\pm$  SEM; n= 4).

### R451C NLGN3-Venus shows reduced secretion and increased degradation rate

To further characterize the newly generated cell-system, we compared basal levels of fluorescence in the medium of WT and R451C NLGN3-Venus selected clones and found a consistent and significant reduction of the R451C NLGN3-

Venus protein secretion (~50%) compared to the WT protein (Fig. 2A), that was also confirmed by western blot analysis (Fig. 2B). To assess if the reduced levels of the R451C NLGN3-Venus are due to degradation through the ERAD, as it was previously shown for the full-length protein (De Jaco et al., 2010), we blocked the proteasome with the inhibitor MG132 and observed the accumulation of the mutant protein in the cell, not detectable for the WT protein (Fig. 2C-D).

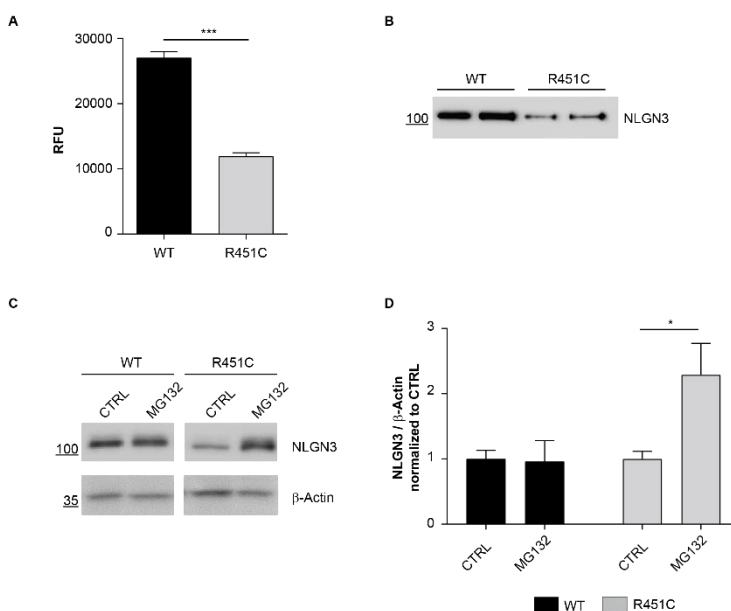


## Figure 2. Characterization of WT and R451C NLGN3-Venus selected clones

A. Fluorescence levels (RFU) in medium from WT and R451C NLGN3-Venus expressing cells (mean  $\pm$  SEM; n= 12; P<0.001; Mann Whitney test).

B. Representative western blot of NLGN3-Venus levels in medium from WT and R451C expressing cells.

C. NLGN3-Venus levels in the medium from WT and R451C expressing cells after treatment with MG132 or in untreated condition.

D. Densitometric analysis of NLGN3 protein levels in the lysates after treatment with MG132, normalized and compared (for each genotype) to untreated control condition (mean  $\pm$  SEM; n= 4; one-way ANOVA \*P< 0.05).

### **ER-retained R451C NLGN3-Venus activates UPR**

Previous work from our group showed the activation of all three branches of the UPR in the PC12 Tet-On cell system with inducible expression of R451C NLGN3 (Ulbrich et al., 2016). Thus, we studied UPR activation in the newly-generated cell system by investigating ATF6 activity by luciferase assay. HEK293 cells expressing either WT or R451C NLGN3-Venus were transfected with a reporter using the Firefly luciferase gene under the control of the ERSE (ER stress sequence elements), found in the promoter of ATF6-target genes. Co-transfection with a Renilla luciferase reporter has been used to assess transfection efficiency. Cells expressing R451C NLGN3-Venus showed significantly higher activation levels of ATF6 compared to WT (Fig. 3).

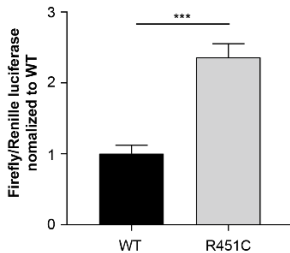


### Figure 3. UPR activation in HEK293 NLGN3-Venus cells

ATF6 activation in HEK293 cells expressing either WT or R451C NLGN3-Venus, shown as ratio Firefly/Renilla luciferases normalized and compared to WT condition (mean  $\pm$  SEM; n= 6; Student's t-test \*\*\*P< 0.001).

### 4-PBA improves NLGN3-Venus trafficking

It is notable that known chemical chaperones, such as 4-PBA, can stabilize protein folding and increase protein trafficking *in vitro* (Uggenti et al., 2016). We treated WT and R451C NLGN3-Venus expressing cells with 4-PBA (500  $\mu$ M) and measured fluorescence levels in the medium. We detected a significant increase of fluorescence for the mutant protein, indicating a positive effect of 4-PBA on improving defective protein trafficking and secretion (Fig. 4). However, this increase was observed also in the medium of the cells expressing the WT protein, denoting a generalized effect of this chemical chaperone on protein folding.

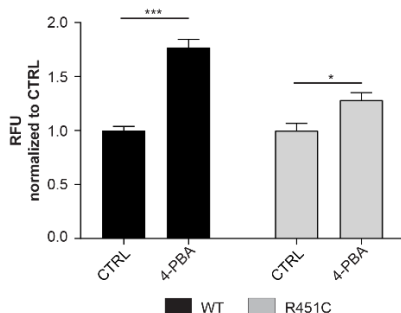


#### **Figure 4. Effects of 4-PBA on WT and R451C NLGN3-Venus expressing cells**

Fluorescence levels (RFU) after treatment with 4-PBA (500  $\mu$ M), normalized and compared (for each genotype) to untreated control condition (mean  $\pm$  SEM; n= 12; one-way ANOVA \*P<0.05 \*\*\*P<0.001).

#### **Screening of an FDA-approved library of compounds**

A library of 2662 compounds was screened for enhancing secretion of mutant R451C NLGN3-Venus protein. All the compounds were previously approved by the American Food and Drugs Administration (FDA) for treatment of a variety of neurological and non-neurological diseases.

The screening was performed at a concentration of 2  $\mu$ M on HEK293 cells expressing R451C NLGN3-Venus. The fluorescence in the medium was measured after 60 hours from treatment, to allow the mutant protein to accumulate to levels detectable by a fluorimeter. From this initial screening, we selected 12 compounds, which showed a 2-fold increase in the fluorescence levels in comparison to the untreated condition

(Fig. 5A). It is noteworthy that most of these compounds belonged to the glucocorticoid family, which is known to increase the levels of ER-resident chaperones (Das et al., 2013).

See supplementary Fig. 1 for a more detailed list of positive compounds.

To confirm data obtained in this first screening and to exclude that some contaminants were present in the library and were interfering with the results, we performed a second screening using a new batch of each compound. However, we chose only 5 of them, 3 glucocorticoids (Prednisolone sodium phosphate, Desonide, Alclometazone dipropionate) and 2 belonging to other chemical families (Quinestrol, Phenytoin sodium) (Table 1) for this further characterization. We tested them on both WT and R451C NLGN3-Venus cells and DMSO was used as vehicle control condition. Only treatments with glucocorticoids showed to significantly increase trafficking of the mutant protein in comparison to control untreated condition, while Quinestrol and Phenytoin sodium had no effect, such as DMSO (Fig. 5C). Glucocorticoids had no effect on the WT NLGN3-Venus (Fig. 5B), indicating a specific effect of the compounds only on the mutant form of the protein.

The significant increase in protein secretion was confirmed by western blot analysis on the cell media (Fig. 6A). It is noteworthy that the amount of NLGN3-Venus protein was unchanged in cell lysates after treatment (Fig. 6B). This was indicating that treatment didn't affect protein synthesis but rather induced a higher proportion of R451C NLGN3-Venus protein to be released in the cell medium.

Name	Fold	Chemical class
Alclometazone dipropionate	2.154262	glucocorticoid
Betamethasone acetate	2.109327	glucocorticoid
Carbenoxolone sodium	2.52415	glycyrrhetic acid derivate with a steroide-like structure
Desonide	2.204494	glucocorticoid
Desoxymetasone	2.383413	glucocorticoid
Ethylnorepinephrine hydrochloride	2.075011	norepinephrine derivate
Isoflupredone acetate	2.371147	glucocorticoid
Milnacipran hydrochloride	2.042192	phenylacetic acids derivate
Phenylethyl alcohol	2.074689	alcohol
Phenytoin sodium	2.189134	imidazole derivate
Prednisolone sodium phosphate	2.475187	glucocorticoid
Quinestrol	2.238747	synthetic estrogen

**Table 1**

Selected compounds that resulted positive from the first screening. The amount of increased fluorescence in the cell medium of R451C NLGN3-Venus expressing cells and the chemical class to which the single compounds belong are indicated.

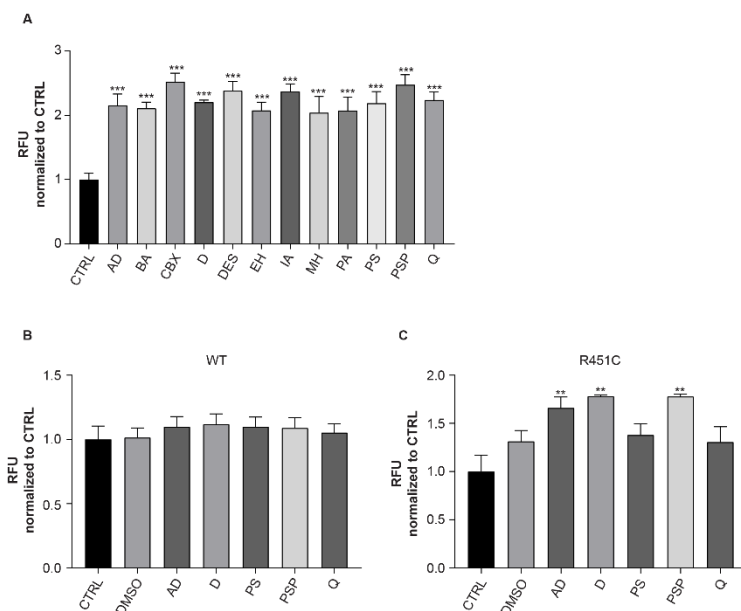


### Figure 5. Screening of an FDA-approved library of compounds

AD: alclometazone dipropionate; BA: betamethasone acetate; CBX: carbenoxolone sodium; D: desonide; DES: desoxymetazone; EH: ethylnorepinephrine hydrochloride; IA: isoflupredone acetate; MH: milnacipran hydrochloride; PA: phenylethyl alcohol; PS: phenytoin sodium; PSP: prednisolone sodium phosphate; Q: quinestrol

A. Fluorescence levels (RFU) in the medium of HEK293 R451C NLGN3-Venus treated with indicated compounds, normalized and compared to untreated control condition (CTRL) (mean  $\pm$  SEM; n= 4; one-way ANOVA \*\*\*P<0.001).

B. Fluorescence levels (RFU) in the medium of HEK293 expressing WT NLGN3-Venus treated with selected compounds or with vehicle control (DMSO), normalized and

compared to control condition (CTRL) (mean  $\pm$  SEM; n= 7; one-way ANOVA).

C. Fluorescence levels (RFU) in the medium of HEK293 expressing R451C NLGN3-Venus treated with selected compounds or with vehicle control (DMSO), normalized and compared to control condition (CTRL) (mean  $\pm$  SEM; n= 7; one-way ANOVA \*\*P<0.01).

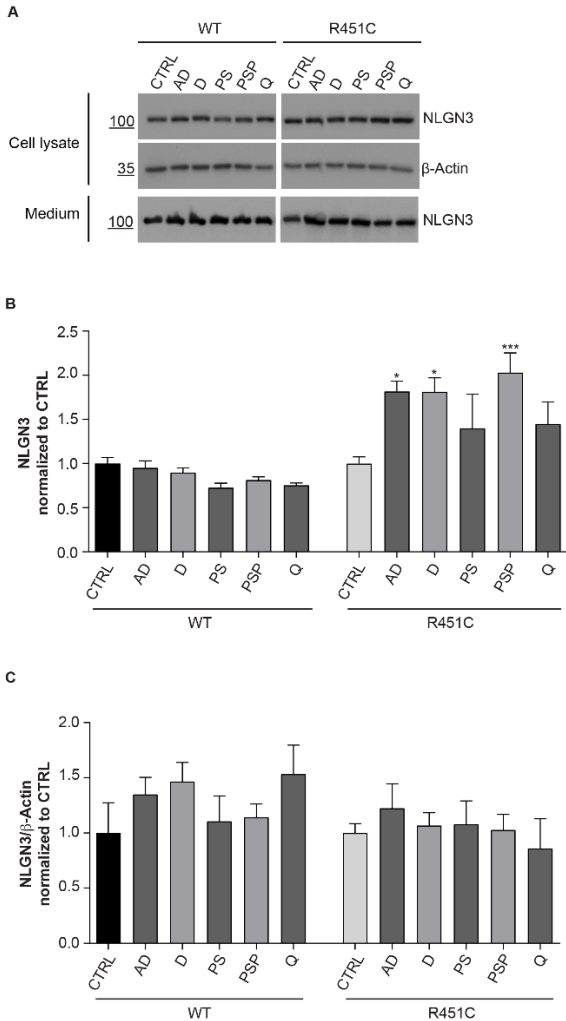


**Figure 6. Quantification of NLGN3-Venus protein after treatment**

AD: alclometazone dipropionate; D: desonide; PS: phenytoin sodium; PSp: prednisolone sodium phosphate; Q: quinestrol

A. Representative western blot of NLGN3-Venus levels in cell lysates and in medium from WT and R451C expressing cells after treatment with indicated compounds

B. Densitometric analysis of NLGN3-Venus levels in cell medium from WT and R451C expressing cells after treatment with indicated compounds, normalized and compared to CTRL condition (mean  $\pm$  SEM; n= 4; one-way ANOVA \*P<0.05 \*\*P<0.01).

C. Densitometric analysis of NLGN3-Venus levels in cell lysates from WT and R451C expressing cells after treatment with indicated compounds, normalized and compared to CTRL condition (mean  $\pm$  SEM; n= 4; one-way ANOVA).

### **Selected compounds improve trafficking of full-length R451C NLGN3**

Compounds selected for enhancing trafficking of the truncated and fluorescent form of NLGN3 were then tested on cells expressing the full-length form of the protein. HEK293 cells were transiently transfected with the pcDNA3.1 vector encoding for R451C NLGN3 full-length and co-localization staining with the ER marker calreticulin was analyzed by confocal microscopy (Fig. 7A) in order to evaluate the exit of the mutant R451C protein from the ER. The effect of the compounds to decrease the amount of co-localization was used as a parameter of their activity. HEK293 cells transiently transfected with WT NLGN3 full-length normally expressed on the cell surface were used as control. As expected, this condition showed a significant lower co-localization with calreticulin in comparison to cells expressing mutant NLGN3 (Fig. 7B). R451C NLGN3 expressing cells were treated with 5

of the selected compounds and co-localization with calreticulin was assessed 48 h after treatment. We considered as positive those compounds able to decrease all three coefficients calculated. It was confirmed that Alclometazone dipropionate and Prednisolone sodium phosphate, resulted the most effective in improving trafficking of both the truncated and full-length R451C NLGN3 mutant forms. The remaining compounds seem not to have any effect on decreasing ER-localization of the full-length mutant protein (Fig. 7C-D-E).

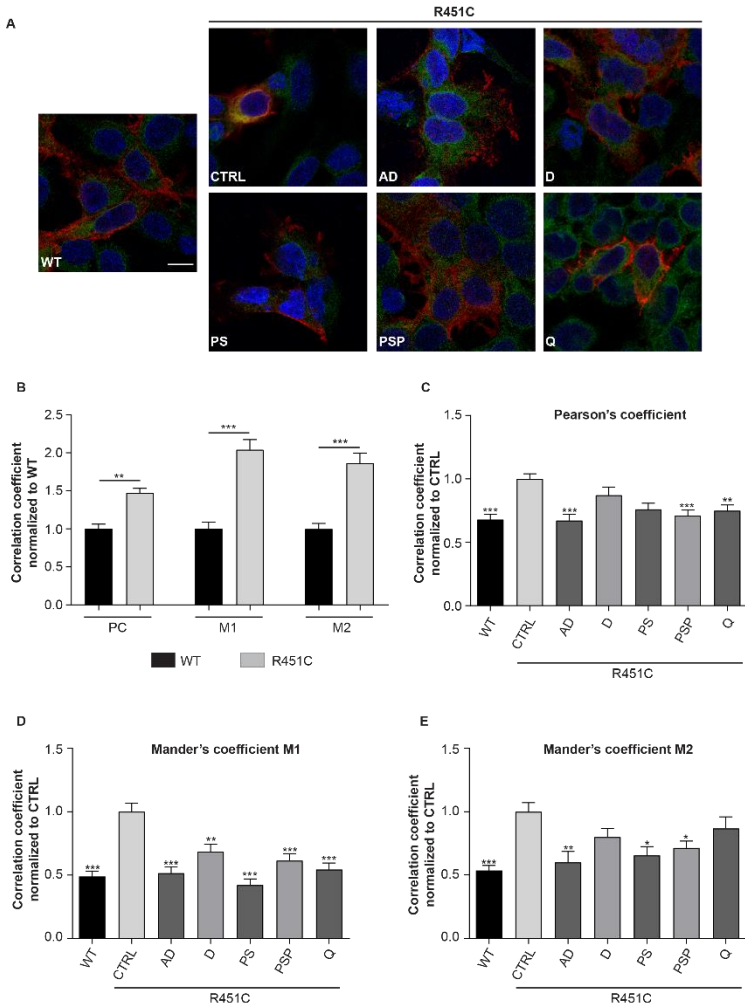


**Figure 7. Compounds effect on localization of full length NLGN3**

AD: alclometazone dipropionate; D: desonide; PS: phenytoin sodium; PSP: prednisolone sodium phosphate; Q: quinestrol

A. Representative confocal images of NLGN3 (red) and Calreticulin (green) staining in HEK293 cells transfected with either WT or R451C NLGN3 treated with selected compounds (scale bar 1  $\mu$ m).

B. Quantification of NLGN3-calreticulin co-localization in cells expressing either WT or R451C NLGN3, normalized and compared to WT condition. Pearson's coefficient (PC) and both Mander's overlap coefficients M1 and M2 were measured (mean  $\pm$  SEM; n= 54 cells/3 independent experiments; one-way ANOVA \*\*P<0.01 \*\*\*P<0.001).

C. Pearson's coefficient measured in cells expressing either WT or R451C NLGN3 and treated with indicated compounds, normalized and compared to CTRL condition (mean  $\pm$  SEM; n= 50 cells/3 independent experiments; one-way ANOVA \*\*P<0.01 \*\*\*P<0.001).

D. Mander's overlap coefficient M1 analysis in cells expressing either WT or R451C NLGN3 and treated with indicated compounds, normalized and compared to CTRL condition (mean  $\pm$  SEM; n= 50 cells/3 independent experiments; one-way ANOVA \*\*P<0.01 \*\*\*P<0.001).

E. Analysis of Mander's overlap coefficient M2 in cells expressing either WT or R451C NLGN3 and treated with indicated compounds, normalized and compared to CTRL condition (mean  $\pm$  SEM; n= 55 cells/3 independent experiments; one-way ANOVA \*P<0.05 \*\*P<0.01).

### **Compounds fail to lower UPR activation induced by full length R451C NLGN3**

We evaluated the effect of the compounds on alleviating UPR activation due to the retention of the full length R451C

NLGN3 in the ER. To this purpose, we used the UPR reporter that measures the activation of the ATF6 branch. HEK293 cells were transiently transfected with pcDNA3.1 expressing full length NLGN3, either WT or R451C, and with the luciferase reporter vectors previously used (Fig. 3). Cells expressing R451C NLGN3 were treated with 5 selected compounds and luciferase activity was measured, in each condition, 48 h after treatment. HEK293 cells expressing WT NLGN3 represented the control condition. The treatment with the compounds failed to decrease the activation of ATF6 in cells expressing R451C NLGN3 comparing to untreated condition (Fig. 8).

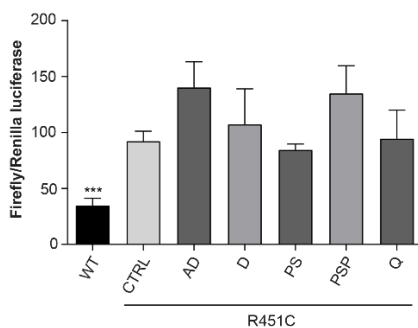


### Figure 8. Effects of compounds on UPR activation

AD: alclometazone dipropionate; D: desonide; PS: phenytoin sodium; PSP: prednisolone sodium phosphate; Q: quinestrol  
Firefly/Renilla luciferases activities in HEK293 cells expressing either WT or R451C NLGN3 and treated with indicated compounds, compared to CTRL condition (mean  $\pm$  SEM; n= 5; one-way ANOVA).

## **Discussion**

In the last years, the research field on diseases correlated to the accumulation of misfolded proteins has been greatly expanding. Collectively called protein-misfolding diseases, they include common neurological and non-neurological disorders, such as Alzheimer's, Parkinson's, Cystic Fibrosis, Cancer and Diabetes (Koss and Platt, 2017; Sarvani et al., 2017; Scheper and Hoozemans, 2016). In these disorders, the common underlying mechanism is represented by the accumulation of misfolded proteins. The ER is specialized in recognizing and retaining not properly folded proteins that undertake the secretory pathway. This might result in a double effect: a loss-of-function due to the mis-localization of the protein, and the accumulation of the protein in the organelle leading to a toxic gain-of-function and in most cases to ER stress conditions. In this contest, the research for small molecules facilitating protein folding and their escape from the ER is becoming of growing interest. Chemical chaperones are useful tools in helping protein folding, but their lack of specificity limits their potential as therapeutics. On the other hand, pharmacological chaperones have a higher specificity, being designed to bind a selected protein (Cortez and Sim, 2014).

Our work focused on the biological effects caused by the Arg451 to Cys substitution (R451C) in the extracellular domain of the post-synaptic protein Neuroligin3 (NLGN3). This mutation, found in patients with ASDs, causes the retention of the protein in the ER and its loss at the synapse, where it plays a crucial role as a cell-adhesion molecule (Baig et al., 2017). Our recent work established the first evidence

between the retention of the R451C NLGN3 in the ER and the activation of UPR *in vitro* (Ulbrich et al., 2016). Moreover, mice carrying the R451C mutation in the endogenous *NLGN3* gene show altered neurotransmission in several brain areas correlated to ASDs (Tabuchi et al., 2009; Etherton et al., 2001; Trobiani et al., 2018). However, it is not clear if those alterations are due to the loss of NLGN3 proper localization on the cell surface, or if it is a consequence of the ER stress condition due to the retention of the protein in the organelle (Trobiani et al., 2018). In fact, it is possible that, in almost completely absence of NLGN3 on the cell surface, the pre-synaptic partner NRXN1 $\beta$  associates with other ligands, thus inducing a gain-of-function. Besides, this hypothesis does not exclude the possibility that the UPR, induced by the ER-retention of R451C NLGN3, represents an additional factor participating to the gain-of-function phenotype.

The effect of restoring proper protein localization to rescue phenotype, has been shown by Mei and colleagues in the Shank3:Cre conditional Knock-In (KI) mouse, a model of ADSs (Mei et al., 2016). Untreated mice showed a phenotype characterized by molecular, electrophysiological and behavioural alterations. Treatment with Tamoxifen activates the Cre-recombinase and re-establishes expression of Shank3 at the post-synaptic site, allowing an almost complete recovery of the phenotype. Therefore, restoration of proper protein expression and cellular disposition might represent a strategy to treat diseases characterized by protein mis-localization.

In this prospective, helping the mutant R451C NLGN3 to exit the ER would be beneficial in two ways: restoring proper protein localization for its function, and alleviating the overload of the ER, reducing ER stress and UPR activation.

We generated stable cell lines expressing a truncated form of either WT or R451C NLGN3, tagged with the fluorescent protein Venus and demonstrated that their trafficking was impaired similarly to what was previously shown for the full-length form of the protein (De Jaco et al., 2006, 2010). We report a ~50% reduction of R451C protein release compared to the WT, increased protein levels following the inhibition of proteasome activity and activation of the UPR. Our cell model system responded to the treatment with 4-PBA, as showed by the increase of protein trafficking for both WT and R451C NLGN3-Venus proteins, suggesting a generalized effect of 4-PBA on all proteins passing through the ER. However, our interest was focused on identifying compounds selective for the mutant R451C NLGN3 form.

We screened a library of compounds, approved by the FDA for treatment of a variety of other diseases. The screening used a concentration 250-fold lower than the one used for 4-PBA and closer to normally used pharmacological concentrations. We found 12 compounds able to enhance R451C NLGN3-Venus trafficking, doubling its amount in the cell medium. It is noteworthy that those compounds had no effect on trafficking of the WT NLGN3-Venus. Two out of the three compounds which resulted the most effective on the truncated NLGN3-Venus, Alclometazone dipropionate and Prendisolone sodium phosphate, showed a specific activity in reducing the retention of the full-length protein in the ER.

Unfortunately, none of the compounds showed an effect at reducing the activation of the ATF6 branch of the UPR caused by the retention of the full-length R451C NLGN3 in the ER. However, it is possible that they modulate other branches of this cellular response or that the amount of mutant NLGN3

escaping from the ER in response to treatment, is not enough to reduce ER stress and UPR activation. Although, the selective effect on the mutant NLGN3, with no effect on the WT form, is indicating that the compounds were not affecting the generalized protein trafficking through the secretory pathway. Instead, they were improving protein folding, probably by increasing levels of ER chaperones (Das et al., 2013; Fujii et al., 2006). It has been shown both *in vitro* and *in vivo*, that the administration of exogenous glucocorticoids, was able to increase levels of ER chaperones, such as Calreticulin, BiP and Hsp70, and induce the escape of an ER-retained protein from this organelle (Das et al., 2013; Duzgun et al., 2013; Fujii et al., 2006; Nair et al., 2018). Moreover, it has been shown that dexamethasone, a synthetic glucocorticoid used in clinic, has a role in modulating the half-life of CFTR by attenuating its interaction with a ubiquitin E3 ligase *in vitro* (Caohuy et al., 2009).

Glucocorticoids mediate their effects by binding the intracellular receptor GR, which translocates to the nucleus and activates transcription of target genes, by binding specific glucocorticoids response elements (GREs) (Meijsing 2015). By this way, glucocorticoids regulate several cellular processes.

In this contest, our findings strongly suggest a role for glucocorticoids in the regulation of protein folding and trafficking and establish a new prospective for treatment of misfolding protein diseases and for the monogenic form of autism due to the R451C substitution in the synaptic protein NLGN3.

Based on these data, in the next future, we aim at elucidating the mechanism of action of glucocorticoids for improving

protein trafficking in our model systems. Moreover, we want to investigate the ability of glucocorticoids at increasing NLGN3 protein expression *in vivo*. Besides, we want to assess the activity of these compounds on other mutant proteins, in order to verify whether this effect is specific for the R451C NLGN3 or is common to ER-retained proteins that are not structurally correlated.



## **Methods**

### **Plasmids generation**

Truncated rat NLGN3 was generated by introducing a stop codon right after the residue Tyr640 in the cDNA encoding for full-length NLGN3 either WT or carrying the mutation Arg451Cys (R451C). The cDNAs were subcloned into a vector encoding an N-terminal FLAG octopeptide and were additionally tagged at the C-terminus with Venus, an analog of the Green Fluorescent protein.

### **Selection of stable clones of HEK293 cells expressing truncated NLGN3-Venus**

pcDNA3.1 plasmid, encoding truncated NLGN3-Venus either WT or R451C, has been used for transfecting HEK293 cells, using polyethylenimine (PEI) procedure (Sigma-Aldrich). Transfected cells were cultured in selective medium composed by DMEM (Dulbecco's Modified Eagle's Medium, Sigma), 5% Fetal Bovine Serum (FBS, Sigma-Aldrich) and 500 µg/ml Geneticin (G418, Corning). Resistant cells have been plated at clonal density in 96-well plate and expanded to obtain clones, which were screened for NLGN3 protein expression by quantifying fluorescence levels in the culture medium and by Western blot on both cell lysates and medium. Stable cell lines are maintained in medium containing 500 µg/ml G418 at 37°C and 5% CO<sub>2</sub>.

The proteasome-inhibitor MG132 (Z-Leu-Leu-Leu-al, #C2211 Sigma-Aldrich) at concentration of 2.5 µM was added in the medium for the last 48 h of culture before harvesting.

## **Luciferase assay**

To assess ATF6 activation, 800.000 HEK293 cells were seeded in a 6-well plate. At 24 h after plating, cells were transfected with 2 µg of total DNA according to the Lipofectamine2000 protocol (Thermo Fisher Scientific). For HEK293 cells stably expressing NLGN3-Venus, total DNA was represented by two vectors: pATF6(5 x)-Luc (Firefly) and pTK (Renilla) in a 50:1 ratio (Davies et al., 2009). Otherwise, besides these two reporter vectors, pcDNA3.1 expressing full length NLGN3, either WT or R451C, was added to the transfection mix. Moreover, in the latter case, 3 h after transfection, HEK293 cells expressing R451C NLGN3 were treated with selected compounds at 2 µM concentration.

Transfection was carried out for 48 h, then cells were harvested and activity of both luciferases was assessed by the Dual-luciferase Reporter Assay kit (Promega) and detected by the Glomax multi+ detection system (Promega).

## **Treatment with chemical chaperones**

HEK293 cells expressing either WT or R451C NLGN3-Venus were plated at a density of 600.000 cells in 24-well plate. 24 h after seeding, medium was changed to Optimem (Gibco) and sodium 4-phenylbutyrate (4-PBA, Sigma-Aldrich) was added at the concentration of 500 µM in the cell culture medium.

For the screening of the FDA-approved compounds, 75.000 cells from both lines have been plated in 96-well plate, in 150 µl Optimem medium added with 2% FBS.

The 2662 compounds of the library were dissolved in 10% DMSO (Sigma-Aldrich) and used at final concentration of 2 µM. Compounds were added in the cell culture medium 24

hours after seeding and fluorescence levels were measured after 60 h of treatment. Cells treated with 0,3% DMSO were used as vehicle control.

### **Quantification of protein secretion by fluorimetric measurements**

To evaluate NLGN3-Venus protein trafficking, 100 µl of medium from cells either untreated or treated with selected compounds was transferred in a black 96-well plate and fluorescence was measured by a fluorimeter (excitation wavelength 485 nm, emission wavelength 535 nm).

### **Preparation of protein samples**

Lysates of HEK293 cells were obtained using lysis buffer (150 mM NaCl, 10 mM Tris pH 8.0, 0.5% Nonidet P40) supplemented with proteases inhibitor cocktail (Sigma-Aldrich). Lysis was performed for 15 min on ice, followed by centrifugation at 17000 g for 15 min at 4°C. Protein concentration in the samples was determined by the Bradford assay.

### **SDS-PAGE and Western blot**

Equal amount of cell medium or 30 µg of cell lysate from NLGN3-Venus (WT or R451C) cells were subjected to SDS-PAGE (10% v/v polyacrylamide gel) in running buffer (25 mM Tris pH 8.3, 0.19 M Glycine, 0.1% Sodium dodecyl sulfate) and transferred to PVDF membrane (Merck-Millipore) in transfer buffer (25 mM Tris pH 8.3, 0.19 M Glycine, 10%

Methanol). The membrane was blocked with 5% w/v non-fat milk in PBS (2.68 mM KCl, 1.47 mM KH<sub>2</sub>PO<sub>4</sub>, 0.137 M NaCl, 10.16 mM Na<sub>2</sub>HPO<sub>4</sub>) and stained with anti-FLAG M2 (1:1000, mouse, Sigma-Aldrich #F3165) or anti-β-Actin (1:1000, mouse, Millipore #MAB1501) primary antibodies diluted in PBS containing 1% BSA (Sigma-Aldrich). HRP (horseradish peroxidase)-conjugated anti-mouse (goat, Sant Cruz Biotechnologies #SC-2005) secondary antibody was diluted 1:10000 in 5% milk in PBS. All the incubations were performed for 1 h at room temperature. The HRP signal has been detected by using ECL (HyGLO, Denville Scientific Inc.) and visualised by a ChemiDoc system (BioRad).

### **Immunocytochemistry**

HEK293 cells (100.000 cells/well) were plated on glass coverslips coated with 0.5 mg/ml poly-D-lysine (Sigma-Aldrich) in 24-well plates. Cells were transfected with cDNA NLGN3 full-length either WT or R451C using the calcium phosphate method and treated with selected compounds for 48 h. Untreated cells cultured in the same conditions were used as control. Cells were washed with PBS and fixed with 4% paraformaldehyde (PFA, Sigma-Aldrich) for 20 minutes at room temperature, followed by fixation with pre-chilled methanol (Sigma-Aldrich) for 15 minutes at -20°C.

The blocking step was performed for 1 h at room temperature using a solution containing 2% normal sheep serum (NSS), 0.1% Triton-X100, 0.02% sodium azide in PBS. The same solution has been used for diluting primary and secondary antibodies. Anti-FLAG (1:5000, Rabbit, Sigma-Aldrich #F7425) and anti-calreticulin (1:500, Mouse, Enzo ADI-

SPA601) were incubated in combination, overnight at 4°C, while fluorescent secondary antibodies Cy3-anti-rabbit (donkey, Jackson Immuno Research #711-165-152) and Alexa Fluor 488-anti-mouse (donkey, Jackson Immuno Research #715-545-151) were diluted 1:500 and incubated 1 h at room temperature. Nuclei were stained with Hoechst (Thermo Fisher Scientific) 1:1000 in PBS for 10 min. Fluorescent signal was detected by confocal microscope (Zeiss) at 63x magnification and co-localization analysis was obtained on Z-stack images using the JACoP plugin of the NIH software ImageJ as previously described (Bolte and Cordelières, 2006). Pearson's correlation coefficient and Mander's overlap coefficients M1 and M2 have been calculated for at least 15 cells/experiment.

### **Statistical analysis**

All experiments were performed at least three times on independent biological samples, as indicated in the figure legends. Student's t-test, Mann Whitney test and one-way ANOVA with Bonferroni multiple comparison test were used for statistical analysis by using Prism5 (Graph-Pad 5 Software Inc.): \*p<0.05, \*\*p<0.01, \*\*\*p<0.001.



## References

- Almanza A, Carlesso A, Chintha C, Creedican S, Doultisinos D, Leuzzi B, Luís A, McCarthy N, Montibeller L, More S, Papaioannou A, Püschel F, Sassano ML, Skoko J, Agostinis P, de Bellerocche J, Eriksson LA, Fulda S, Gorman AM, Healy S, Kozlov A, Muñoz-Pinedo C, Rehm M, Chevet E, Samali A (2018). Endoplasmic reticulum stress signalling - from basic mechanisms to clinical applications. *FEBS J.* Epub ahead of print
- Baig DN, Yanagawa T, Tabuchi K (2017). Distortion of the normal function of synaptic cell adhesion molecules by genetic variants as a risk for autism spectrum disorders. *Brain Res Bull.* 129, 82-90
- Bang ML, Owczarek S (2013). A matter of balance: role of neurexin and neuroligin at the synapse. *Neurochem Res.* 38(6), 1174-89
- Bemben MA, Shipman SL, Nicoll RA, Roche KW (2015). The cellular and molecular landscape of neuroligins. *Trends Neurosci.* 38(8), 496-505
- Bolte S, Cordelières FP (2006). A guided tour into subcellular colocalization analysis in light microscopy. *J Microsc.* 224(Pt 3), 213-32
- Campisi L, Imran N, Nazeer A, Skokauskas N, Azeem MW (2018). Autism spectrum disorder. *Br Med Bull.* 127(1), 91-100
- Caohuy H, Jozwik C, Pollard HB (2009). Rescue of DeltaF508-CFTR by the SGK1/Nedd4-2 signaling pathway. *J Biol Chem.* 284(37), 25241-53

Chambers JE, Marciniak SJ (2014). Cellular mechanisms of endoplasmic reticulum stress signaling in health and disease. 2. Protein misfolding and ER stress. *Am J Physiol Cell Physiol.* 307(8), C657-70

Christensen J, Grønberg TK, Sørensen MJ, Schendel D, Parner ET, Pedersen LH, Vestergaard M (2013). Prenatal valproate exposure and risk of autism spectrum disorders and childhood autism. *JAMA.* 309(16), 1696-703

Comoletti D, De Jaco A, Jennings LL, Flynn RE, Gaietta G, Tsigelny I, Ellisman MH, Taylor P (2004). The Arg451Cys-neurotrophin-3 mutation associated with autism reveals a defect in protein processing. *J Neurosci.* 24(20), 4889-93

Corazzari M, Gagliardi M, Fimia GM, Piacentini M (2017). Endoplasmic Reticulum Stress, Unfolded Protein Response, and Cancer Cell Fate. *Front Oncol.* 7, 78

Cortez L, Sim V (2014). The therapeutic potential of chemical chaperones in protein folding diseases. *Prion.* 8(2)

Crider A, Ahmed AO, Pillai A (2017). Altered Expression of Endoplasmic Reticulum Stress-Related Genes in the Middle Frontal Cortex of Subjects with Autism Spectrum Disorder. *Mol Neuropsychiatry.* 3(2), 85-91

Das I, Png CW, Oancea I, Hasnain SZ, Lourie R, Proctor M, Eri RD, Sheng Y, Crane DI, Florin TH, McGuckin MA (2013). Glucocorticoids alleviate intestinal ER stress by enhancing protein folding and degradation of misfolded proteins. *J Exp Med* 210(6), 1201-16

Davies MJ, Miranda E, Roussel BD, Kaufman RJ, Marciniak SJ, Lomas DA (2009). Neuroserpin polymers activate NF-

kappaB by a calcium signaling pathway that is independent of the unfolded protein response. *J Biol Chem.* 284(27), 18202-9

De Jaco A, Comoletti D, Kovarik Z, Gaietta G, Radic Z, Lockridge O, Ellisman MH, Taylor P (2006). A mutation linked with autism reveals a common mechanism of endoplasmic reticulum retention for the alpha,beta-hydrolase fold protein family. *J Biol Chem.* 281(14), 9667-76

De Jaco A, Dubi N, Comoletti D, Taylor P (2010). Folding anomalies of neuroligin3 caused by a mutation in the alpha/beta-hydrolase fold domain. *Chem Biol Interact.* 187(1-3), 56-8

De Jaco A, Lin MZ, Dubi N, Comoletti D, Miller MT, Camp S, Ellisman M, Butko MT, Tsien RY, Taylor P (2010). Neuroligin trafficking deficiencies arising from mutations in the alpha/beta-hydrolase fold protein family. *J Biol Chem.* 285(37), 28674-82

De Jaco A, Dubi N, Camp S, Taylor P (2012). Congenital hypothyroidism mutations affect common folding and trafficking in the  $\alpha/\beta$ -hydrolase fold proteins. *FEBS J.* 279(23), 4293-305

de la Torre-Ubieta L, Won H, Stein JL, Geschwind DH (2016). Advancing the understanding of autism disease mechanisms through genetics. *Nat Med.* 22(4), 345-61

Di Prisco GV, Huang W, Buffington SA, Hsu CC, Bonnen PE, Placzek AN, Sidrauski C, Krnjević K, Kaufman RJ, Walter P, Costa-Mattioli M (2014). Translational control of mGluR-dependent long-term depression and object-place learning by eIF2 $\alpha$ . *Nat Neurosci.* 17(8), 1073-82

Duzgun A, Bedir A, Ozdemir T, Nar R, Kilinc V, Salis O, Alacam H, Gulden S (2013). Effect of dexamethasone on unfolded protein response genes (MTJ1, Grp78, Grp94, CHOP, HMOX-1) in HEp2 cell line. *Indian J Biochem Biophys.* 50(6), 505-10

Etherton M, Földy C, Sharma M, Tabuchi K, Liu X, Shamloo M, Malenka RC, Südhof TC (2011). Autism-linked neuroligin-3 R451C mutation differentially alters hippocampal and cortical synaptic function. *Proc Natl Acad Sci U S A.* 108(33), 13764-9

Fabrichny IP, Leone P, Sulzenbacher G, Comoletti D, Miller MT, Taylor P, Bourne Y, Marchot P (2007). Structural analysis of the synaptic protein neuroligin and its beta-neurexin complex: determinants for folding and cell adhesion. *Neuron.* 56(6), 979-91

Falivelli G, De Jaco A, Favaloro FL, Kim H, Wilson J, Dubi N, Ellisman MH, Abrahams BS, Taylor P, Comoletti D (2012). Inherited genetic variants in autism-related CNTNAP2 show perturbed trafficking and ATF6 activation. *Hum Mol Genet.* 21(21), 4761-73

Fujii Y, Khoshnoodi J, Takenaka H, Hosoyamada M, Nakajo A, Bessho F, Kudo A, Takahashi S, Arimura Y, Yamada A, Nagasawa T, Ruotsalainen V, Tryggvason K, Lee AS, Yan K (2006). The effect of dexamethasone on defective nephrin transport caused by ER stress: a potential mechanism for the therapeutic action of glucocorticoids in the acquired glomerular diseases. *Kidney Int.* 69(8), 1350-9

Giepmans BN, Adams SR, Ellisman MH, Tsien RY (2006). The fluorescent toolbox for assessing protein location and function. *Science*. 312(5771), 217-24

Halperin L, Jung J, Michalak M (2014). The many functions of the endoplasmic reticulum chaperones and folding enzymes. *IUBMB Life*. 66(5), 318-26

Hillary RF, FitzGerald U (2018). A lifetime of stress: ATF6 in development and homeostasis. *J Biomed Sci*. 25(1), 48

Jamain S, Quach H, Betancur C, Råstam M, Colineaux C, Gillberg IC, Soderstrom H, Giros B, Leboyer M, Gillberg C, Bourgeron T; Paris Autism Research International Sibpair Study (2003). Mutations of the X-linked genes encoding neuroligins NLGN3 and NLGN4 are associated with autism. *Nat Genet*. 34(1), 27-9

Kawada K, Mimori S (2018). Implication of Endoplasmic Reticulum Stress in Autism Spectrum Disorder. *Neurochem Res*. 43(1), 138-143

Kawada K, Mimori S, Okuma Y, Nomura Y (2018). Involvement of endoplasmic reticulum stress and neurite outgrowth in the model mice of autism spectrum disorder. *Neurochem Int*. 119, 115-119

Koss DJ, Platt B (2017). Alzheimer's disease pathology and the unfolded protein response: prospective pathways and therapeutic targets. *Behav Pharmacol*. 28(2 and 3-Spec Issue), 161-178

Kosuge Y, Sakikubo T, Ishige K, Ito Y (2006). Comparative study of endoplasmic reticulum stress-induced neuronal death

in rat cultured hippocampal and cerebellar granule neurons. *Neurochem Int.* 49(3), 285-93

Li X, Zou H, Brown WT (2012). Genes associated with autism spectrum disorder. *Brain Res Bull.* 88(6), 543-52

Martella G, Meringolo M, Trobiani L, De Jaco A, Pisani A, Bonsi P (2018). The neurobiological bases of autism spectrum disorders: the R451C-neuroigin 3 mutation hampers the expression of long-term synaptic depression in the dorsal striatum. *Eur J Neurosci.* 47(6), 701-708

Martínez G, Vidal RL, Mardones P, Serrano FG, Ardiles AO, Wirth C, Valdés P, Thielen P, Schneider BL, Kerr B, Valdés JL, Palacios AG, Inestrosa NC, Glimcher LH, Hetz C (2016). Regulation of Memory Formation by the Transcription Factor XBP1. *Cell Rep.* 14(6), 1382-1394

Martínez G, Khatiwada S, Costa-Mattioli M, Hetz C (2018). ER Proteostasis Control of Neuronal Physiology and Synaptic Function. *Trends Neurosci.* 41(9), 610-624

McQuiston A, Diehl JA (2018). Recent insights into PERK-dependent signaling from the stressed endoplasmic reticulum. *F1000Res.* 6, 1897

Mei Y, Monteiro P, Zhou Y, Kim JA, Gao X, Fu Z, Feng G (2016). Adult restoration of Shank3 expression rescues selective autistic-like phenotypes. *Nature.* 530(7591), 481-4

Meijnsing SH (2015). Mechanisms of Glucocorticoid-Regulated Gene Transcription. *Adv Exp Med Biol.* 872, 59-81

Mercado G, Castillo V, Soto P, Sidhu A (2016). ER stress and Parkinson's disease: Pathological inputs that converge into the secretory pathway. *Brain Res.* 1648(Pt B), 626-632

Mihailidou C, Panagiotou C, Kiaris H, Kassi E, Moutsatsou P (2016). Crosstalk between C/EBP homologous protein (CHOP) and glucocorticoid receptor in lung cancer. *Mol Cell Endocrinol.* 436, 211-23

Mizukami T, Orihashi K, Herlambang B, Takahashi S, Hamaishi M, Okada K, Sueda T (2010). Sodium 4-phenylbutyrate protects against spinal cord ischemia by inhibition of endoplasmic reticulum stress. *J Vasc Surg.* 52(6), 1580-6

Hebert DN, Molinari M (2007). In and out of the ER: protein folding, quality control, degradation, and related human diseases. *Physiol Rev.* 87(4), 1377-408

Nair M, Romero J, Mahtabfar A, Meleis AM, Foty RA, Corbett SA (2018). Dexamethasone-Mediated Upregulation of Calreticulin Inhibits Primary Human Glioblastoma Dispersal Ex Vivo. *Int J Mol Sci.* 19(2)

Nakanishi M, Nomura J, Ji X, Tamada K, Arai T, Takahashi E, Bućan M, Takumi T (2017). Functional significance of rare neuroligin 1 variants found in autism. *PLoS Genet.* 13(8), e1006940

Ni H, Rui Q, Xu Y, Zhu J, Gao F, Dang B, Li D, Gao R, Chen G (2018). RACK1 upregulation induces neuroprotection by activating the IRE1-XBP1 signaling pathway following traumatic brain injury in rats. *Exp Neurol.* 304, 102-113

Nosyreva E, Kavalali ET (2010). Activity-dependent augmentation of spontaneous neurotransmission during endoplasmic reticulum stress. *J Neurosci.* 30(21), 7358-68

Ozcan U, Yilmaz E, Ozcan L, Furuhashi M, Vaillancourt E, Smith RO, Görgün CZ, Hotamisligil GS (2006). Chemical chaperones reduce ER stress and restore glucose homeostasis in a mouse model of type 2 diabetes. *Science*. 313(5790), 1137-40

Qi X, Hosoi T, Okuma Y, Kaneko M, Nomura Y (2004). Sodium 4-phenylbutyrate protects against cerebral ischemic injury. *Mol Pharmacol*. 66(4), 899-908

Ribeiro LF, Verpoort B, de Wit J (2018). Trafficking mechanisms of synaptogenic cell adhesion molecules. *Mol Cell Neurosci*. 91, 34-47

Roussel BD, Kruppa AJ, Miranda E, Crowther DC, Lomas DA, Marciniak SJ (2013). Endoplasmic reticulum dysfunction in neurological disease. *Lancet Neurol*. 12(1), 105-18

Sarvani C, Sireesh D, Ramkumar KM (2017). Unraveling the role of ER stress inhibitors in the context of metabolic diseases. *Pharmacol Res*. 119, 412-421

Scheper W, Hoozemans JJ (2015). The unfolded protein response in neurodegenerative diseases: a neuropathological perspective. *Acta Neuropathol*. 130(3), 315-31

Südhof TC (2017). Synaptic Neurexin Complexes: A Molecular Code for the Logic of Neural Circuits. *Cell*. 171(4), 745-769

Südhof TC (2008). Neuroligins and neurexins link synaptic function to cognitive disease. *Nature*. 455(7215), 903-11

Sun L, Zhao Y, Zhou K, Freeze HH, Zhang YW, Xu H (2013). Insufficient ER-stress response causes selective mouse

cerebellar granule cell degeneration resembling that seen in congenital disorders of glycosylation. *Mol Brain*. 6, 52

Tabuchi K, Blundell J, Etherton MR, Hammer RE, Liu X, Powell CM, Südhof TC (2007). A neuroligin-3 mutation implicated in autism increases inhibitory synaptic transmission in mice. *Science*. 318(5847), 71-6

Takayanagi S, Fukuda R, Takeuchi Y, Tsukada S, Yoshida K (2013). Gene regulatory network of unfolded protein response genes in endoplasmic reticulum stress. *Cell Stress Chaperones*. 18(1), 11-23

Talebizadeh Z, Lam DY, Theodoro MF, Bittel DC, Lushington GH, Butler MG (2006). Novel splice isoforms for NLGN3 and NLGN4 with possible implications in autism. *J Med Genet*. 43(5), e21

Taoufik E, Kouroupi G, Zygianni O, Matsas R (2018). Synaptic dysfunction in neurodegenerative and neurodevelopmental diseases: an overview of induced pluripotent stem-cell-based disease models. *Open Biol*. 8(9)

Trobiani L, Favaloro FL, Di Castro MA, Di Mattia M, Cariello M, Miranda E, Canterini S, De Stefano ME, Comoletti D, Limatola C, De Jaco A (2018). UPR activation specifically modulates glutamate neurotransmission in the cerebellum of a mouse model of autism. *Neurobiol Dis*. 120, 139-150

Tsai PT (2016). Autism and cerebellar dysfunction: Evidence from animal models. *Semin Fetal Neonatal Med*. 21(5), 349-55

Ugenti C, Briant K, Streit AK, Thomson S, Koay YH, Baines RA, Swanton E, Manson FD (2016). Restoration of mutant

bestrophin-1 expression, localisation and function in a polarised epithelial cell model. *Dis Model Mech.* 9(11), 1317-1328

Ulbrich L, Favaloro FL, Trobiani L, Marchetti V, Patel V, Pascucci T, Comoletti D, Marciniak SJ, De Jaco A (2016). Autism-associated R451C mutation in neuroligin3 leads to activation of the unfolded protein response in a PC12 Tet-On inducible system. *Biochem J.* 473(4), 423-34

Valenzuela V, Martínez G, Duran-Aniotz C, Hetz C (2016). Gene therapy to target ER stress in brain diseases. *Brain Res.* 1648(Pt B), 561-570

Valenzuela V, Jackson KL, Sardi SP, Hetz C (2018). Gene Therapy Strategies to Restore ER Proteostasis in Disease. *Mol Ther.* 26(6), 1404-1413

Williams ME, de Wit J, Ghosh A (2010). Molecular mechanisms of synaptic specificity in developing neural circuits. *Neuron.* 68(1), 9-18

Yan J, Oliveira G, Coutinho A, Yang C, Feng J, Katz C, Sram J, Bockholt A, Jones IR, Craddock N, Cook EH Jr, Vicente A, Sommer SS (2005). Analysis of the neuroligin 3 and 4 genes in autism and other neuropsychiatric patients. *Mol Psychiatry.* 10(4), 329-32

## Supplementary

Plate	Fold	Drug Name	Plate	Fold	Drug Name
1B11	1.716692	Methylprednisolone	14H4	2.189134	Phenytin sodium
2B11	1.723117	Flurandrenolide	14H11	1.5842	Chloroacetoxyquinoline
2C4	1.515889	Flunisolide	15H10	1.219024	Benazepril hydrochloride
2C5	1.481229	Flumethasone	16C4	1.190505	Pyritione zinc
2H6	1.737316	Hydrocortisone valerate	17C2	1.4064	Trimetazidine dihydrochloride
3A3	1.743062	Betamethasone valerate	17D2	1.503258	Phthalylsulfacetamide
4F3	1.340454	Betamethasone	17G8	1.513433	Dichlorisone acetate
5D9	1.614775	Dexamethasone	18D8	1.513768	Methylprednisolone sodim succinate
6A3	1.551375	Estriol	21B9	1.381591	Decitabine
6A4	1.556175	Estrone	21D4	1.48628	Bethametasone dipropionate
6A5	1.603917	Ethacrynic acid	21D5	1.68889	Bortezomib
6A6	1.763019	Ethambutol hydrochloride	22F4	1.532698	Hydrocortisone (cortisol)
6A7	1.550549	Ethinyl estradiol	22G7	1.492684	Loteprednol Etabonate
8A2	1.84651	Triamcinolone	22H7	1.300689	Esomeprazole sodium
8A3	1.761748	Triamcinolone acetonide	24A2	1.269405	Clomiphene citrate (Z, E)
9G11	1.763401	Betamethasone 17,21-dipropionate	24A9	1.328269	Daunorubicin hydrochloride
10H4	2.006945	Sirolimus	24E6	1.576652	Hydrocortisone base
11A5	1.2742	Trifluridine	24H10	1.255238	Fexofenadine HCl
11D4	2.154262	Alclometazone dipropionate	25B6	1.541501	6 $\alpha$ -Methylprednisolone acetate
11E10	1.53454	Prednicarbate	25B8	1.458504	6 $\alpha$ -Methyl-17 $\alpha$ -hydroxy-progesterone
12B9	1.506997	Prednisolone hemisuccinate	25H4	1.732663	Beclomethasone
12D3	1.253051	Doxorubicin	26C5	1.469945	Bucladesine sodium
12G10	2.109327	Betamethasone acetate	27B10	1.338585	Triamcinolone acetonide acetate
12H10	2.383413	Desoxymetasone	27B11	1.336509	Clindamycin phosphate
12H3	1.284427	Epirubicin hydrochloride	27D11	1.332829	Cyclazocine
12H7	2.475187	Prednisolone sodium phosphate	27H2	1.489881	Diffucortolone pivalate
13A4	2.371147	Isoflupredone acetate	27H3	1.417274	Diffuprednate
13A11	2.204494	Desonide	28H9	1.459426	Flumethasone pivalate
13E10	1.400105	Mometasone furoate	28H10	1.498454	Fluocinolone acetonide 21-acetate
13G6	1.534334	Sotalol hydrochloride	28H11	1.542837	Fluorometholone acetate
13G7	1.564321	Mycophenolate mofetil	34A11	1.465726	Prednisolone 21-phosphate disodium
14A4	2.52415	Carbenoxolone sodium			
14A9	1.412271	Tegaserod maleate			
14B4	2.238747	Quinestrol			
14D3	2.074689	Phenylethyl alcohol			
14D10	2.075011	EthylInorepinephrine hydrochloride			
14E3	1.961175	Flucatisone propionate			
14F3	2.042192	Milnacipran hydrochloride			
14H2	1.650591	Phenazopyridine hydrochloride			

## Supplementary Fig. 1

List of the top 69 compounds selected from the screening.



## General conclusions and perspectives

Several neurological and non-neurological diseases can be ascribed to mutations causing alterations of the three-dimensional structure of the involved proteins (Mercado et al., 2016; Corazzari et al., 2017). According to the severity of the misfolding, proteins can be retained in the ER and degraded. The consequence of this process is a loss-of-function, due to the lack of proper protein localization. However, the accumulation of misfolded proteins in the ER can induce a gain-of-function, due to the activation of the UPR (Almanza et al., 2018). Indeed, besides its role in responding to stress and re-establishing ER homeostasis, UPR plays a role in modulating several aspects of cell physiology. This is of particular interest in the brain, where it has been demonstrated that UPR can regulate synaptic function (Di Prisco et al., 2014; Nosyreva and Kavalali, 2010).

In this context, a consistent field of research is focusing on developing treatments for improving protein folding therefore alleviating ER stress.

Our interest is focused on the biological effects of the ASDs-associated mutation R451C in the synaptic protein NLGN3. This mutation maps in the extracellular domain, causing a local misfolding of this protein region, which leads to an almost complete retention of NLGN3 in the ER in several cellular model systems (De Jaco et al., 2010; Ulbrich et al., 2016).

In my PhD thesis I have conducted two strictly correlated studies, both focused on the R451C mutation. The first concerned the effects of the mutation *in vivo* and the second relates to the development of an *in vitro* approach for studying

strategies to rescue NLGN3 folding defects caused by the mutation.

The *in vivo* approach used the knock-in (KI) mouse model endogenously expressing the R451C NLGN3 protein (Tabuchi et al., 2007). My work has demonstrated that the R451C mutation induced protein instability and ER-retention in the total brain of the KI mouse, similarly to what has been demonstrated *in vitro*, causing an increase in its degradation rate in comparison to the parental WT strain (Trobiani et al., 2018). This is the first study that analyzed the expression of the mutant protein during development. Moreover, my work showed that the effects caused by the mutation were detectable already during development at the embryonic stage E18, supporting the role of NLGN3 in synapses assembly and maturation (Williams et al., 2010). Interestingly, we observed UPR activation selectively in the cerebellum both at embryonic and adult stages. Remarkably, we have shown that it caused alterations of the synaptic functions, influencing the release of glutamate from the pre-synaptic terminal (Trobiani et al., 2018). This result fits with the current literature proposing a role for the UPR in regulating physiological function of the nervous system (Di Prisco et al., 2014; Martinez et al., 2016, 2018).

The selective impairment of the cerebellum rather than other brain regions can be explained by the higher sensitivity of this region to stress (Kosuge et al., 2006; Sun et al., 2013). Therefore, our data provide evidence for a gain-of-function effect of the R451C mutation *in vivo* and establish a link between UPR and the ASDs phenotype. Moreover, our results strengthen the importance of dysfunction of the cerebellum in neurodevelopmental disorders. In fact, the implication of the

cerebellum in the pathogenesis of ASDs has been highlighted by both clinical and preclinical studies. Moreover, several genes whose mutations have been associated to ASDs are highly expressed in the cerebellum, such as the Neuroligins (Tsai, 2016).

The second aim of my work was focused on developing an *in vitro* approach, to fish a commercial library for chemical compounds improving mutant NLGN3 protein folding. We have generated cell lines expressing a truncated and fluorescent form of NLGN3 consisting of the extracellular domain, protein region where most of the autism-linked mutations are found. We have used this system to study the trafficking of R451C NLGN3, however in the future this strategy could be applied for studying other autism-linked mutations or to study the R451C homologous mutations in acetylcholinesterase, butyrylcholinesterase or thyroglobulin (De Jaco et al., 2006, 2012).

The screening of a library of chemical compounds, using this newly generated cell system, identified several members of the glucocorticoid family showing activity in rescuing the trafficking of R451C mutant protein and reducing its ER-retention. Although these glucocorticoids do not influence the ATF6 branch of the UPR, this is not excluding that they might act on other branches of this response or through a different mechanism. However, it is noteworthy that these glucocorticoids showed an effect only on the mutant form of the protein, with no effect on the WT form of NLGN3. This is indicating that their action is not generalized on all proteins undertaking the secretory pathway, but that it is specific of misfolded ones. This might be due to the previously demonstrated ability of glucocorticoids to increase levels of

ER chaperones in conditions of ER stress (Das et al., 2013). In this case, chaperones would have an effect only on the misfolded protein rather than on the WT, which is already correctly folded.

Considering the data I have obtained so far, the future prospective will investigate the role of glucocorticoids in regulating protein trafficking in order to reveal the mechanism of action. Indeed, it is known that they can increase levels of ER chaperones and, in some cases, modulating the interaction between a ubiquitin E3 ligase and its protein target (Duzgun et al., 2013; Caohuy et al., 2009).

Afterward, it would be interesting to test their efficacy *in vivo*, by determining whether the treatment improve R451C NLGN3 protein stability in the brain of the KI mouse model. Moreover, glucocorticoids could be tested for alleviating the functional alterations induced by the UPR in the cerebellum. In fact, a direct interaction between glucocorticoids, their receptor and members of the UPR cascade has been previously demonstrated (Duzgun et al., 2013; Mihailidou et al., 2016).

In order to generalize the effect of these compounds on acting on protein folding, it would be necessary to investigate the activity of glucocorticoids on other misfolded proteins whose mutations induce ER-retention, but that are structurally not correlated to NLGN3, such as Caspr2 (Falivelli et al., 2012).

This would elucidate whether they are potentially useful for any ER-retained locally misfolded protein such as the R451C mutation in NLGN3.

To conclude, our work is part of a new and intriguing field of research, which aims to find a possible treatment for diseases correlated with protein misfolding, most of which have been untreatable so far. Moreover, it supports the contribution of the

synaptic pathway in the etiology of ASDs. In fact, we have shown that a decreased trafficking of a synaptic protein and its retention in the ER, due to a misfolding mutation, impairs synaptic transmission in a specific brain area. Our work contributes to a better understanding of the molecular mechanisms underlying the ASDs pathogenesis.



## LIST OF PUBLICATIONS

- **Trobiani L.**, Favaloro F.L., Di Castro M.A., Di Mattia M., Cariello M., Miranda E., Canterini S., De Stefano M.E., Comoletti D., Limatola C., De Jaco A. (2018)  
*UPR activation specifically modulates glutamate neurotransmission in the cerebellum of a mouse model of autism.*  
Neurobiology of disease
- Di Bari M., Bevilacqua V., De Jaco A., Laneve P., Piovesana R., **Trobiani L.**, Talora C., Caffarelli E., Tata A.M. (2018)  
*Mir-34a-5p Mediates Cross-Talk between M2 Muscarinic Receptors and Notch-1/EGFR Pathways in U87MG Glioblastoma Cells: Implication in Cell Proliferation.*  
International journal of molecular sciences
- Martella G., Meringolo M., **Trobiani L.**, De Jaco A., Pisani A., Bonsi P. (2018)  
*The neurological bases of Autism Spectrum Disorders: The R451C-Neurexins 3 mutation hampers the expression of long-term synaptic depression in the dorsal striatum*  
European Journal of Neuroscience
- Ulbrich L., Favaloro F.L., **Trobiani L.**, Marchetti V., Patel V., Pascucci T., Comoletti D., Marciniak S., De Jaco A. (2016)  
*Autism associated R451C mutation in Neurexins3 leads to the activation of the unfolded protein response in a PC12 Tet-On inducible system*  
Biochemical Journal

- Favaloro F.L., Ulbrich L., **Trobiani L.**, Cariello M., De Jaco A. (2015)  
*Linking endoplasmic reticulum stress to neurodevelopmental disorders*  
European Journal of Histochemistry